UNIVERSITY OF CALIFORNIA

SANTA CRUZ

CONSTRUCTION OF LOW COST MULTILAYERED SOFT ROBOTS CONTAINING EMBEDDED INTRINSICALLY SOFT SENSORS

A thesis submitted in partial satisfaction of the
requirements for the degree of

MASTER OF SCIENCE

in

ELECTRICAL AND COMPUTER ENGINEERING
by

Conrad M Esch

June 2020

The Thesis of Conrad M Esch
is approved:

Professor Michael Wehner, Chair

Professor Gabriel Hugh Elkaim

Professor Miercea Teodorescu

Quentin Williams
Acting Vice Provost and Dean of Graduate Studies

Contents

List of Figures

List of Tables

Nomenclature

C	Capacitor Value
F_r	Square wave frequency, driven by R_s
f_s	Square wave frequency, driven by R_s
k	$\frac{R1}{R1+R2}$
$R1$	Resistor 1
$R2$	Resistor 2
R_s	Sensor Impedance
v	Voltage
1E3MES	1-Ethyl-3-methylimidazolium ethyl sulfate
DAC	Digital to Analog Converter
EGaIn	Eutectic gallium-indium alloy
PCB	Printed Circuit Board
PSI	Pounds per Square Inch

Abstract

Construction of Low Cost Multilayered Soft Robots Containing Embedded Intrinsically Soft Sensors

by

Conrad M Esch

Soft robotics as a new and emerging field has the potential to become an integral part in the area of robotics by providing new methods of interacting with environments not capable through conventional robotics. However, soft robot's nonlinear nature can be difficult to both control and model. This paper will present several examples of modern soft robotic applications and solutions. A novel construction method for embedded, intrinsically soft sensors as a part of a more significant actuator system will be shown. This was accomplished by employing the use of low cost components and tools including a spin coater and a vacuum chamber. This actuator was made using both Ecoflex 00-30 [9] and Dragonskin 10 [7] silicone rubber with the goal being to maximize sensor responsitivity without compromising useful grip strength. The sensor is composed entirely of an ionic liquid [20] whose fluidic nature makes it intrinsically soft and an ideal sensor medium for soft robots. The ionic liquid is captured inside of continuous sensor channels that are molded into the layers of the actuator. These channels are sampled by taking advantage of the change in impedance of the liquid as its cross sectional area and length increases or decreases. To be able to accurately measure this change without breaking down the ionic fluid, the sensors are integrated as a resistor into a relaxation oscillator

where the output frequency is driven by the change in impedance of the sensor. The equation $P_s = \frac{R_s}{3.891*10^8}$ describes this relationship where P_s is the output period of a square wave and R_s is the impedance of the sensor. The actuator was integrated into a matching mount system that was designed to securely hold the actuator and provide strain relief for the 4 wires and single air supply tube. These wires and tube connect the actuator to its support system, shown in figure 0.1, which is necessary to both sample the integrated sensors on and control the actuator. The actuator system is evaluated from the viewpoint of both sensor responsitivity and sensitivity to changes in input pressure. Results will be shown and discussed that demonstrate the effectiveness of both the bend and force sensors. The complete actuator system was then integrated into a feedback control loop, which allowed the actuator to track a ramp reference signal. This was made possible through the characterization of the actuator which resulted in a 4th order polynomial representing the relationship between input pressure and bend sensor output. Finally, suggestions will be made for further research to increase the overall usefulness of this system in an effort to increase the cumulative research impact of this design.

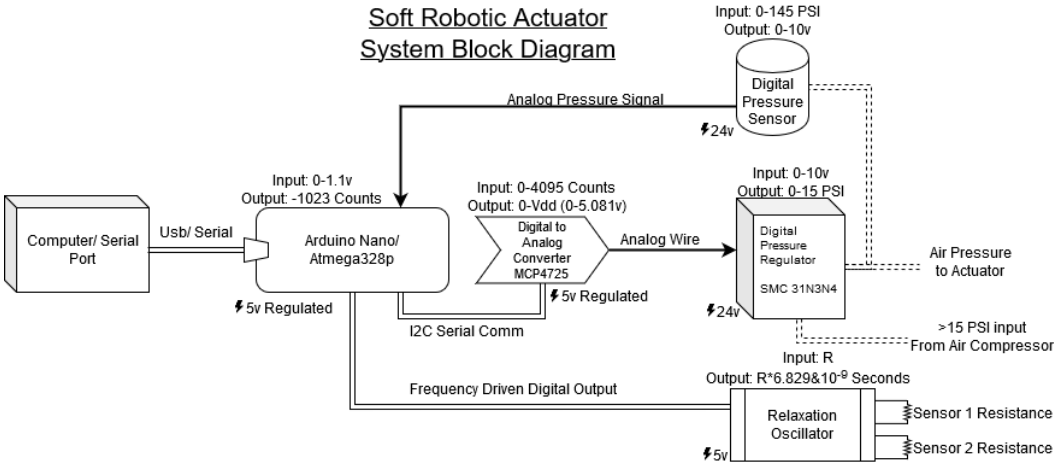

Figure 0.1: **This figure shows the complete system setup need to collect data from one of the actuators. The central component of the system is the Arduino Nano which was used for both controlling the actuator and for taking data in from it's sensors. This data was then sent via serial port to the computer.**

Acknowledgments

My thanks go to Professor Michael Wehner for his advisement, guidance, and support. I would also like to thank my reading committee, Professors Gabe Elkaim and Mircea Teodorescu, I also thank the numerous people that have helped to make this endeavour possible. Special thanks to Keng-yu Lin who provided incredibly helpful advice and was always available to discuss ideas with. Megan Boivin was helpful in working to define and develop the goals of this research as well as the feedback controller. Cris Vasquez and Arturo Gamboa-Gonzalez helped me build numerous actuators especially toward the end of the project. Aviv Elor, Joe Adamson, and Megan Boivin were instrumental in providing editting for my thesis. I would also like to thank Teodorescu Lab and Victoria Ly for donating their time and 3D printing resources which were used to create the actuator molds.

Chapter 1

Background

1.1 Motivation

Soft robotics is a new and emerging field which proponents characterize as having unlimited potential due to the current lack of soft robotic applications in industry with some exceptions [26]. Ostensibly the term soft robotics describes any form of a transducer which incorporates soft components, these soft components can be made of almost any non rigid material but often are comprised of silicon rubbers, Polydimethylsiloxane (PDMS), fabrics, and other flexible but not necessarily stretchable materials. Due realative newness of research into soft robotics and the current interest in it, the definition of what precisely is a soft robot is not clearly defined. In addition, previous research projects incorporating soft materials could considered "soft robots" but at the time they di not not label themselves as such due to the fact that the term itself "soft robot" did not come into use until the early 1980's ([11]). Much of modern soft robotics research can be attributed to developments

in soft materials from research into products such as contact lenses or other soft products that have to conform to humans.

1.1.1 Soft Robotics for Exploration

Soft Robots are actively being researched for the purposes of scientific and disaster exploration. Such robots could have the ability to traverse uneven surfaces while being able to squeeze around or under obstacles. This is due to their inherently non rigid nature.

One project at NASA Langley sought to explore whether soft robots could be used in space or on the surface of Mars or the Moon [13]. Specifically they explored whether soft robots could be used for either assembly of structures or exploration of other planets. In a description of their goals, they stated "The first is mobility, looking into how the actuator is able to move. For example, moving across the lunar surface. Joining, as the second key property, is vital to understanding exploring how the robots would interlock and link together. Two soft robots could connect together to produce a large temporary shelter" [13]. The article was written at the beginning of their research and as such doesn't go into great detail about the results of their investigation. The takeaway is that NASA considers investigating soft robots as used in space exploration as a worthy endeavour.

In Shepherd et al.'s paper [19], they explored the design of an entirely soft robot that could traverse an area using sophisticated locomotion. As described in the paper it is a "tetrapod" that "can lift any one of its four legs off the ground and leave the other three legs planted to provide stability." [19]. To accomplish this they used

what they referred to as pneumatic channels which is similar to and serves the same purpose as the actuator chambers in this project. These pneumatic channels were actuated in sequence by an off-board set of regulators. For exploration, the authors showed that their robot could navigate under obstacles. This is in comparison to a more conventional hard robot which would not be ably to change its shape in response to an obstacle. Their robot is able to successfully compress itself from it's normal walking height to something much smaller at the cost of overall speed. Further research led to an untethered version [27] which was shown to be durable to impacts, heat, and cold. This is a feature common to silicone and could be an asset in designing future robots for exploration. A downside to this robot is that it didn't feature any form of sensing to know if it came in contact with an object or to know the overall bend of it's legs. A set of sensors could have greatly increased the flexibility and capabilities of this type of robot.

1.1.2 Soft Robotics for Medicine

Medicine is a field filled with potential applications for soft robots. Soft robots are normally composed of materials that are considered medically safe such as silicone and pdms. As such they start out with a head start in material choice for their designs, they also are attractive for medicine due to their flexibility. Surgery and medical procedures can often be rough on the human body, especially with hard stainless steel implements. Due to soft robot's flexible nature, they have the potential to conform to and squeeze through the body. This, in principle, is similar to the multigait robot [19] mentioned above which also used it's flexibility to squeeze

through obstacles.

One project that explored an unconventional use for soft robots was "An actuatable soft reservoir modulates host foreign body response" [6] which explored ways in which soft robots could be used in conjunction with implantable medical devices. The issue the authors wanted to solve was that implantable medical devices can often trigger a response in their host "such as fibrosis and inflamation" [6]. These types of devices can include neural probes, catheters, pacemakers, etc. Their goal was to design a device "that actively modulates the biomechanics of the biotic-abiotic interface by altering strain, fluid flow, and cellular activity" [6]. Essentially, they hoped to change the cells response by massaging the cells using a soft robot. To do this they designed a small reservoir that they could inflate using an external (to the reservoir) pump. This had the general shape of a balloon but on a milliscale. Actuating the reservoir served two purposes, first it guaranteed that the cells of the host would never be in permanent contact with the reservoir, this allowed greater amounts of healthy fluid to flow around the cells and prevent fibrosis. Secondly by leaving the reservoir normally inflated, it allowed the researches to deflate it and create a greater area of dispersal for drugs when using a porous version of the reservoir designed with two fill tubes. Ultimately they proved this was successful but it could of proved more successful if it had incorporated a soft pressure sensor that could provide information about the build up of fibrotic material.

Another more conventional project explored the use of soft robots for surgical applications. The "STIFF-FLOP surgical manipulator: Mechanical design and experimental characterization of the single module" [5] paper presented and explored

the use of inflatable, segmented soft robots as a surgical tool for Minimally Invasive Surgeries. This could be used as a replacement for more conventional tools that rely upon "motors, moving rods, gears, or a combination of cables and rods." [5] The STIFF-FLOP works by having 3 fluid chambers spaced evenly around a "Stiffening Chamber". The 3 fluid chambers are made of a flexible silicone that can be pressurized to bend the actuator in any direction. The stiffening chamber in the middle contains granules that when placed under a vacuum hold their shape. All of this is placed in an accordion style tube that keeps the fluid chambers from bowing out while allowing them to expand along the length of the tube, changing it's shape. This application is incredibly flexible but is theoretically limited in overall length by the number of modules that can be stacked together. While it was certainly effective, applying bend sensors to the STIFF-FLOP could have led to a greater exploration of controllability. This was discussed by another paper [18] which is discussed in a following section.

1.1.3 Soft robotics for Plant Processes and Agriculture

The most common example of a soft robot is that of a gripper. These are commonly made out of a form of silicone and use inflatable chambers along their spine to bend and grip objects. Usually there are multiple fingers arranged facing each other so as to enclose an object. Their flexible construction leads to numerous advantages when gripping objects: primarily, the fact that they are actuated with air and made out of rubbery silicone allows them to wrap around objects. This happens because as they bend sections of the gripper come in contact with objects, and the air inside

the gripper takes the path of least resistance causing sections of the gripper not in contact with an object to bend at a greater angle. This allows grippers to conform to objects with variable or odd shapes. The added bonus to this effect is because they wrap around an object they also apply gripping force at a much higher surface area. This eliminates pressure points caused by solid grippers and can allow soft grippers to grab delicate objects. Much research has gone into soft robotic grippers, including this thesis, but for the sake of brevity only three examples will be discussed.

Soft Robotics Inc ([26]) is to the best of the authors knowledge the only company specializing in and selling soft robotic grippers. They advertise their grippers as being able to lift objects as delicate as a pastry and with rapid speed. This is accomplished because all of the motivation for the gripper can be stored away from the end effector. Other grippers may require electronic components on the end of their industrial armatures, but because soft robotic grippers are driven primarily by air, motivating them is as simple as attaching them to a hose connected to a pressure regulator and compressor. This can theoretically be stored far away from the armature. Overall this reduces the weight of the end effector while the massive amounts of potential energy stored in an air compressor can be almost instantaneously applied to the gripper. They have a modular system of grippers allowing the user to change the spacing, length, and pressure with ease. The one downside to their system is that it seems to be an open loop controller, it observes an object of a certain size and uses a preset amount of pressure to close the gripper on that object. Using both bend and pressure sensors could be advantageous to

making their gripper design more flexible to unknown situations.

Researchers have also explored how to make grippers even more adaptable to unique situations. The paper "Universal soft pneumatic robotic gripper with variable effective length" [12] explores whether being able to lock sections of a gripper can improve it's ability to grip and manipulate an object. They accomplished this by tying off sections of the gripper and then attempting to grip the same object and measuring the force exerted. Overall they showed that this can have a dramatic impact on grip force however they did not fabricate a method to actually implement this in realtime. It shows promise though and could be further enhanced with a force sensor that could indicate the size of an object without having to use a camera.

A final paper of note is "A Prestressed Soft Gripper: Design, Modeling, Fabrication, and Tests for Food Handling" [30]. This paper explores whether manufacturing a set of grippers in such a way that in their relaxed state they are bent outward could allow the gripper to grab large objects. Using similar manufacturing techniques to this thesis, they built the gripper in two parts, a bottom skin attached to an upper actuator chamber. They stretched the actuator chamber portion in a clamp and then glued the skin onto it. When cured, this gave the actuator a curled backwards appearance which was due to the actuator chamber portion wanting to return to it's unstretched state. This would be similar to the appearance and function of applying a vacuum to a conventional gripper. They also developed a standard sized mount for this application and when comparing conventional grippers to their design on this mount they found that the bent outwards grippers could enclose and grip much larger objects. The issue with the conventional gripper was not that it could not

grab the same size objects but more that it could not in its relaxed state fit around the object before actuating. The researchers also compared this to conventional grippers that had been canted outwards at a similar angle to the prestressed grippers. They found that the canted grippers could not grip objects with as much force as the prestressed grippers due to them already using up much of their range of motion just to reach the object.

1.1.4 Future of Soft Robotics

Overall soft robotics currently has infinite potential in the fields of exploration, medicine, and general handling of products. There are many designs that provide a lot of promise but just like the steam engine of old they will need some form of feedback control to fully actualize their potential. To be able to create a feedback loop, some form of data concerning the state of the soft robot is necessary and by extension a sensor will be necessary whether they are cameras or embedded in the robot itself. Inherently soft sensors may be the best option overall because they do not change the dynamics of the robot and they at this point in time can provide a faster data rate at less cost.

1.2 Sensor Technologies and Construction

1.2.1 Capacitive and Magnetic Sensing Technologies

Magnetic and Capacitive sensors represent a lot of potential for soft robots. What makes them highly appealing in concept is that they should be relatively immune

to temperature and moisture and would be mostly a solid state device. This is further enhanced by the fact that there wouldn't need to be any direct electrical connection connection between what could in rudimentary terms be considered the transducer and the effector. In these examples the effector would be the magnet or the outermost plate of the capacitive sensor while the transducer would be a hall effect sensor or the innermost plate.

Researchers have and are actively exploring the use of magnetic sensors in soft robots. One group explored whether a simple magnetic sensor could be used for measuring curvature [16]. Their goal was to design a sensor that could be used for measuring the curvature of a soft robotic snake. Their hardware design was relatively simple, consisting only of an off the shelf hall effect sensor that was soldered onto a flexible pcb. A neodynimium magnet was also attached to the flexible pcb. This formed the basis of their sensor setup which they then placed inside of a piece of silicone. To test their design, they placed the pcb in various sections of a spiral mount that allowed them to vary bend angle. Overall they were successful but acknowledged that their was some noise in their design which limited their sensor rate to 7.5hz. As an outside perspective, one of the aspects of their design which could be limiting in specific situations is that their magnet was mounted onto the flexible pcb with the hall effect sensor. This is fine for a system where part of the soft robot is not intended to stretch, but it could create issues where a robot is supposed to or inadvertently stretches. Besides unknown changes in length, it's possible that this system would still work if the magnet were attached only with silicone.

While magnetic sensors would be good for measuring changes in relative position,

capacitive sensor have the potential to measure force or pressure. There are many different forms that this sensor could take, but most research seeks to make it a component of the robot that is made out of the same materials as the robot itself. One paper, seeking to find the most optimum materials for designing a capacitive sensor compared various common soft robot materials that could function as a dielectric [14]. Their design began with with a conductive lycra material, this is connected to a dielectric, and finally a flexible pcb that allowed them to measure changes in capacitance at individual points. With only 11 points to measure capacitance on the pcb, they could still get a high degree of resolution by combining data from all 11 points [14].

On a related research path, one paper attempted to recreate human touch using a custom built soft capacitive sensor based on PDMS [29]. They stacked PDMS on top of fluorosilicone (a dielectric), which was then stacked onto more PDMS. On the bottom PDMS layers were 4 patches of a conductive textile, arranged in a grid. On the top PDMS layer was a single patch of conductive textile, placed directly in the middle of the 4 bottom patches. The conductive patches served as the plates of the capacitor, where the top patch served as the emitter of the electric signal. This design was incredibly interesting because by using four patches, the researches could detect and measure tangential force on the top layer of PDMS. Just as interesting is that the researchers stated that because of the unique design of the sensor, they were able to measure force with a useful resolution between 0 and 0.6 Newtons and forces up to 12 Newtons. This was due to what the researchers referred to as the 3 dielectrics in their sensor. As normal force is applied to the sensor, the first part

that is compressed is the air gap which naturally occurs due to the fluorosilicone dielectric. The compression of the air gap gave them good resolution between 0 and 2 kpa. After this the fluorosilicone dielectric would be compressed which had a greater resistance to the applied force than the air. Finally the third dielectric was the woven conductive patches which further resisted compression but would yield under force. With all of these aspects combined, the researchers managed to produce a highly responsive and useful capacitive sensor.

1.2.2 Embedded Hard Sensors

Many common off the shelf sensors such as force sensors [10] and resistive bend sensors [25] can be easily integrated into existing soft robotic designs. Typically they are already designed to be flexible in one or two dimensions which can make them an ideal solution for many soft robot designs, especially considering their low cost and high level of design heritage. What is unfortunately typical of these sensors is that they do not stretch like silicone elastomer. This can place limits on their use in designs and may relegate them to sections of a design that are not expected to stretch or deviate in any way from moving on 1 dimension.

One such design focused on using commercial, resistive bend sensors [25] in a soft robot to close a feedback control loop. Their design was essentially a tube containing two Flexible Fluidic Actuators, simliar to the STIFF-FLOP [5] but it could only bend along one plane. They hoped that by placing two bend sensors inside of the actuator, they could measure the overall bend and control it. Their controller was a simple PI controller and ultimately they were successful. They did note that their

actuator module did elongate somewhat under normal operation. They used two flex sensors to overcome this issue, the flex sensor used for feedback was the one opposite of the active FFA, this mitigated the effects on the sensor due to stretching and gave a more accurate reading.

1.2.3 Liquid Sensors

Liquid sensors offer some of the most potential for integration into soft robots which is represented by the wide variety of work that has gone into researching them. They can often take the form of an electrical impedance sensor or a visual sensor. What makes liquid based sensors so promising is that the container that the liquid exists in can be made out the same material as the soft robot itself. This can lead to sensors that have little to no impact on the dynamics of a given soft robot. Liquid's non compressible nature, while different than the more compressible materials such as pdms and silicone can be used as an advantage. Due to it being non compressible, it falls to the designer to design the channels that consistently affect the shape of the liquid. One application used the fact that liquids can't compress to huge advantage. They built a force sensor that uses colored liquid to estimate where force is applied to a surface [24]. When the channels of the force sensor were compressed, the liquid's level move along the tube. This movement is recorded by a camera that can estimate the force applied. This is a really interesting example of a sensor because it requires almost no hardware except for a camera which does not need to be embedded in the device itself.

Probably the most common type of liquid sensor is one that uses some form of

a metal or ionic fluid as a variable impedance sensor. A great example of this is "Design and Fabrication of Soft Artificial Skin Using Embedded Microchannels and Liquid Conductors" [17]. They created a skin that could register force in three axis, specifically they could measure normal force as well as the skin being stretched. To accomplish this they used a manufacturing process that is very similar to the one described in this paper. They used 3d printed molds to create a total of 4 layers of channels out of silicone rubber. They then attached those layers together using a spin coater which spun on more silicone as a glue. Finally they injected EGaIn which is a metal that behaves like a liquid at room temperature but has a low enough conductance to be measurable. This project was incredibly successful and the responsiveness of their skin was very detailed but they did find some non linearity in their response to normal force.

One other paper of note chose not to use a conventional ionic fluid or EGaIn in their sensor [18]. They set out with the goal of developing a sensor that was biocompatible. For this requirement most ionic liquids and EGaIn could not be used due to their toxicity. Instead they chose to go with a saline solution which is biocompatible. This was ultimately combined with glycerol which is considered biocompatible and had the benefit of increasing the saline solution's viscosity which decreased the amount of bubbles in the sensor. Overall the design was effective and specifically the use of a biocompatible saline solution was shown to be effective.

1.2.3.1 Constructing Soft Somatosensitive Actuators via Embedded 3d Printing

The work that had the most bearing on this project was "Soft Somatosensitive Actuators via Embedded 3D Printing" [28], in this paper the authors presented a novel 3d printing technology that had the ability to print sensors into the uncured silicone of soft robots. Essentially this involved taking a negative mold for an actuator and filling it with uncured silicone rubber. A needle attached to some sort of an armature then injects various fluids into the pdms. By carefully choosing the injection path, the researchers could put both sensor fluid, the ionic fluid 1-Ethyl-3-methylimidazolium ethyl sulfate (1E3MES), and what they called a fugitive ink into the actuator. After curing, the sensor fluid would stay in the channels it had displaced during the cure process and the fugitive ink would be extracted out of the actuator leaving a gap for the air chambers. This created a very precisely constructed actuator with almost if not no room for manufacturing errors. To prove the validity of their 3d printing technology, they added multiple sensors to the actuator, including an inflation sensor, two contact sensors, and a bend sensor. Most of these sensors are similar in function to the one's shown in this thesis with the exception of the inflation sensor which was left out due to it's complexity.

While this paper was enormously successful and demonstrated that this 3d printing technique had exceptional promise, there are a few downsides in addition to the high cost of the printer itself. A minor downside is that it would be extremely difficult to design in the robot features that wrap around other features. This would

require the injection needle to possibly pass through an already injected feature which could cause problems. The biggest downside though to this technology is that it requires a high degree of engineering skill to accomplish the construction of an actuator. Both the sensor fluid and the fugitive ink are carefully constructed and made out of multiple materials to make their viscosity easily injectible into the uncured silicone while still making their relative buoyancy equal to the silicone. If the relative buoyancy was different, then the ink could potentially shift up or down during the cure process. The fugitive ink is also interesting in that it was designed so that at low temperatures ($4°c$) it is liquid but at room temperature it is a gel. This meant that to remove the fugitive ink, the actuator had to be cooled and then the ink was extracted using a syringe. With the above in mind, it's clear that although the project demonstrated huge advances in the area of soft robotic fabrication, it was a complicated and potentially expensive build process.

1.2.4 Sensor Technology Conclusion

The results that are contained in the following sections of this thesis draw heavily from the body of work done by other researchers focusing on soft robots and their sensors. Of particular note are "Design and Fabrication of Soft Artificial Skin Using Embedded Microchannels and Liquid Conductors" [17] which used manufacturing techniques which are almost identical to the processes described in the next section with a heavy emphasis on the use of spincoated, uncured silicone to act as a glue in between layers. Also informative was Soft Somatosensitive Actuators via Embedded 3D Printing" [28], who's design and choice of sensor fluid, 1-Ethyl-3-

methylimidazolium ethyl sulfate (1E3MES), which measured both bend and force applied by an actuator was used in this work.

1.3 Conclusions On the Field

Soft robotics has a lot of potential which is evidenced by the wealth of recent research has occurred. Much of this research has gone into applying soft robotics to the fields of exploration [13, 19, 27], product handling [26], and medicine [5, 6], but for these applications to be fully realized Soft Robots will need to become better at sensing their environments. A fair amount of work as presented in the previous section has gone into attempting to integrate sensors into soft robots, with the goal always being to use sensor technologies that do not affect the overall dynamics of the robot. This explains the popularity of liquid sensors for sensing force [24, 17, 18, 28] and bend. A few papers [28] have actually focused on integrating a liquid sensor into some form of motivator such as an actuator but usually they fall short of verifying that it could then be used to control the actuator in a feedback loop. The creation process for these actuators has also tended to be slow and expensive. To advance the field, novel sensor technologies will need to be integrated and tested in broader soft robotic systems. This will allow researchers to begin applying innovative control systems and schemes to motivate soft robots effectively and with precision.

1.4 Project Goals

Based upon the preceding examples, it appears that there is a clear need for soft robotic systems, specifically actuators, that have embedded intrinsically soft sensors. These can then be controlled to a high degree of precision. With this in mind the goals of this project were to provide this type of a system. This project sought to create an actuator with an embedded liquid bend sensor as well as a force sensor to detect contact with objects. This was developed with the requirement that the materials be low cost and the tools be easy to use and procure. The actuator would also need a supporting system consisting of a mount, electronics, and air pressure control. The complete system would need to be fully integrated in such a way that a feedback loop on a microcontroller could change input pressure to the actuator based upon data from the sensors. Finally, it had to be shown that the results were repeatable and the entire system could be constructed from scratch with a high success rate. With these goals in mind, the following section will discuss how the actuator was developed and integrated into a complete and controllable system.

Chapter 2

Development Process

This section will show the development process for the actuator system. First will be covered the evolution of the actuator design itself. Three separate versions were fabricated before landing on a final design. The 3rd and final version is made out of multiple materials in an attempt to increase grip strength without sacrificing sensor responsivitiy. This actuator was integrated into a mount system that securely held it and provided strain relief on the connecting wires. In this section of the thesis the electrical and air systems are also described and documented because they were critical to creating a complete, working system.

2.1 Version 1 - Initial Design

2.1.1 V1 Design Features

The initial design shown in figure 2.1 was an attempt to recreate the success and results of the original paper [28] that this project's design was based on. The decision

was made to forgo the inflation sensor because the manufacturing of this component would require a much more complicated mold system. This left only the top Bend Sensor and the bottom Force sensor as well as the air chambers for motivating the actuator. This resulted in 5 total layers needed to construct the initial design; these layers can be seen in figure 2.2. The height and width of the sensor channel was calculated based upon what was assumed to be the cross sectional area of the sensor channels used in the preceding design. The molds for this design can be seen in figures A.2, A.3, and A.4.

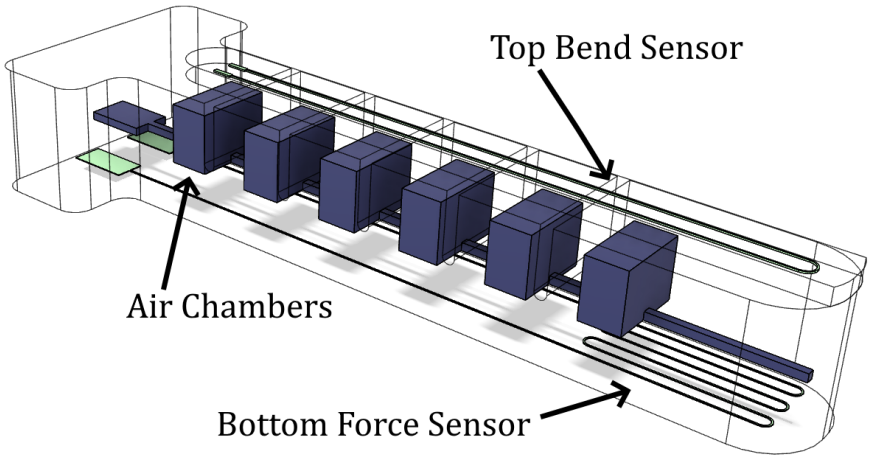

Figure 2.1: **Image of Version 1's complete design with the sensor channels highlighted in green and the air channels highlighted in blue.**

2.1.2 V1 Manufacturing Methods

Manufacturing the actuators for the V1 design was a simple but did not result in success. The actuator was entirely made out of Ecoflex-0030 [9]. A 1 to 1 ratio of

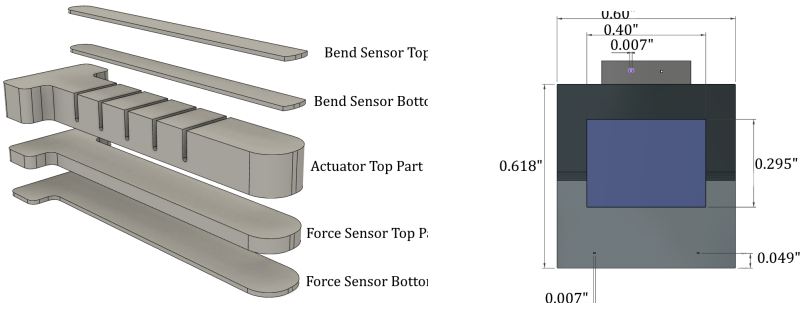

(a) (b)

Figure 2.2: The left image(a) shows how the initial prototype was made using 5 layers of silicone elastomer which required 5 separate molds while the right image (b) shows a cross section of the actuator which details the dimensions of the sensor channels.

Ecoflex-0030 was hand mixed and poured in each of the 5 molds. When filled these were put in a vacuum chamber which was set to -27 PSI to pull any air bubbles out of the Ecoflex-0030. Once bubbles stop appearing at the top level of the mold, the molds were taken out, topped off with more Ecoflex-0030 and then placed in a $60°C$ oven to cure.

Once fully cured, more Ecoflex-0030 was mixed and applied to the interior tops and bottoms of the actuator pieces to act as a glue and bind them together. This was spread on by hand using a wooden applicator.

2.1.3 V1 Results

Overall this design and construction method had a significant amount of drawbacks. Beginning with the molds themselves. The molds were 3D Printed using an SLA printer and standard resin, as a result they had the tendency to warp in the

oven during curing. This had an impact on the final shape of the part post cure. They were also designed to need less time and resin to manufacture and thus most of the parts, especially the lid for the air bladder molds, eventually broke in some way. This part was extremely flimsy and the pegs that were used to hold it in place eventually broke after putting it together and taking it apart multiple times.

The design of the actuator itself had its own problems. The sensor and air channels were overall too shallow. This combined with the crude use of a wooden applicator to spread Ecoflex-0030 onto the surfaces lead to almost every channel having a location where it was filled in with Ecoflex-0030. This made the sensor portion useless because the sensors could not carry current. While in some spots too much silicone was applied, in others too little was applied which led to fluid leaking out between layers. The actuation portion also had problems. The design had few air chambers and they were somewhat large. As a result the potential for blowouts was high. Blowouts are caused by defects along the wall of an air chamber, and can lead to a decreased resistance to pressure in that location which can cause the silicone to become overstretched. This can result in a cascading situation in which a particular chamber will take extra load compared to the other ones.

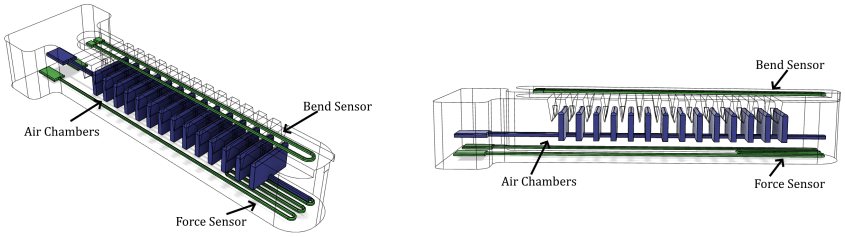

(a) (b)

Figure 2.3: The left and right images (a and b) shows the complete version 2 design with sensor channels highlighted in green and air channels highlighted in blue.

2.2 Version 2 - Improvements to Design for Constructability

2.2.1 V2 Design Features

In terms of general shape and concept, this design shares many common features with the original version. Of significance are the overall length and dimensions. Where its design differs is the air and sensor channels. To make constructibility easier and to prevent the Ecoflex-0030 glue from filling in the sensor channels, the channels were made both wider and taller. Even though the V1 design was not actually tested and thus there is nothing to compare against, this change in the V2 design may have had the added benefit of bring the overall impedance. This should to an increase in sensor sensitivity to changes.

The other main change to this design is in the air bladders themselves. Due to the tendency of the previous version to have blowouts, this version was designed

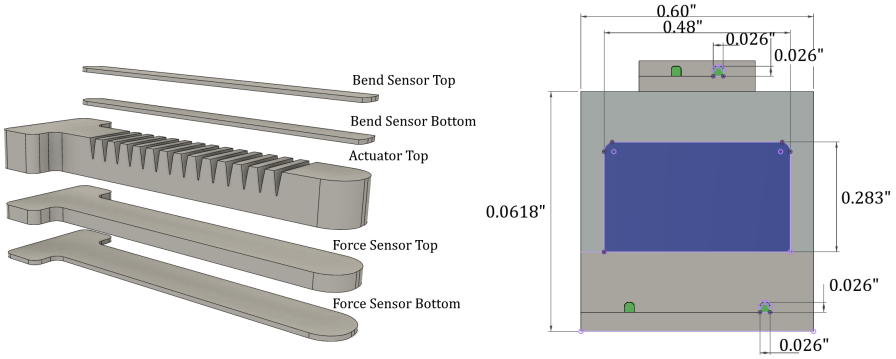

(a) (b)

Figure 2.4: **The left and right images (a) shows the layers composing the design for Version 2 whereas the right image (b) shows a cross sectional image.**

to mitigate those issues. It was designed with more air bladders that were smaller and spaced more tightly together. The goal of this was to have each each chamber expand less than the original while adding more chambers to get the same range of motion. This should make each chamber more resilient to potential defects in the silicone by reducing the chamber volume relative to its wall thickness. In addition, each chamber is also linked to its adjoining chamber for about 2/3 of its height. This will also prevent blowouts by allowing the silicone to press against something physical instead of atmospheric pressure. The final change was to add a rib down the middle of the chamber cutouts, which prevented additional stress being placed on the chambers due to gravity while still allowing the actuator to bend as designed.

2.2.2 V2 Manufacturing Methods

The manufacturing methods for this version of actuator are the same as the previous. The actuator was still constructed using Ecoflex-0030 [9] and the gluing together of the individual components was still done using a wooden applicator. However this process was easier and now pluasible for creating a working actuator due to the increased sensor channel size.

2.2.3 V2 Results

This design was a significant improvement upon the previous. The increased channel size allowed more uncured silicon to be applied using the applicator without filling in the channels. This allowed for the individual layers to be more strongly laminated together. The use of smaller and more numerous air chambers effectively reduced the potential for blowouts and made the whole design more resilient. Even with the design improvements, actually constructing a complete, fully functional actuator took a bit of chance. Even when carefully laminating the layers together there were always a fair amount of failed parts that resulted from sensor channels getting filled in. While this design was effective, it was clear that additional techniques needed to be looked into for laminating the pieces together. As a note, the molds were also strengthened and thickened which prevented warping in the oven. Eventually though the prototypes made from these molds failed due to the gap between the acrylic mount and the top sensor. When the wire was inserted into the top sensor and clamped by the mount, the gap between the two locations would form a stress point on the wire every time an actuation occurred. Eventually this led to

wire breaks. This being the first mostly working prototype, another issue was noted: overall the gripping force of the actuator was quite low. This was due, primarily, to the exclusive use of Ecoflex-0030 [9] in the design. Ecoflex-0030 is extremely flexible and stretchy but that came at the cost of being able to apply useful force.

2.3 Version 3 - Changes in Contruction and Mold Design

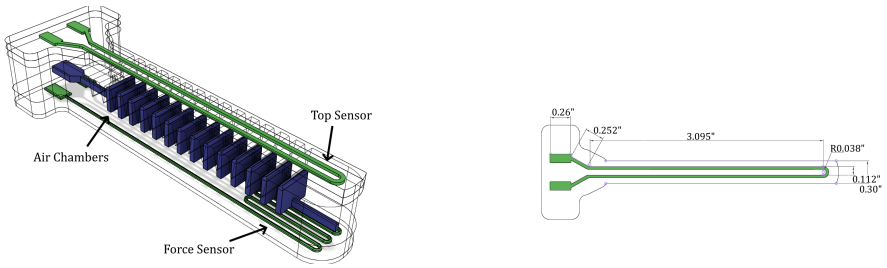

(a) (b)

Figure 2.5: **The left figure (A) shows the complete and final version of the finger that was developed. The right figure (B) shows the only significant change to this actuator, the top sensor was lengthened to place it's sensor fluid reservoirs under the top plate of the mount.**

2.3.1 V3 Final Design Changes

The final design only had one change from version 2: the top sensor was extended so that the sensor fluid reservoirs were located under the actuator mount. This was done to increase the robustness and longevity of the actuator. Placing them there allowed the wires which pierced the reservoirs to be protected under the top part

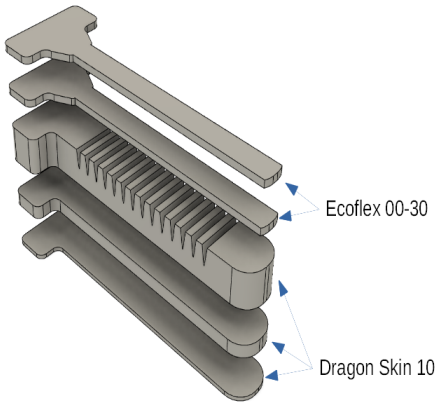

Figure 2.6: **This figure shows the layers for the final version of the actuator that was developed. Of note is that compared to previous versions, this version had an elongated top sensor. It also featured multiple types of silicone rubber which allowed it to retain sensitivity while exerting more force.**

of the actuator mount. This prevented the issue observed in the previous version in which the solid core wires would eventually break due to repeated bending stress as the actuator was inflated.

Also of note is that the materials were changed for some parts of the actuator. In this version the bottom sensor and part containing the air chambers were manufactured using Dragon Skin 10 [7]. This can be seen in figure 2.6. These were in turn attached to a Dragon Skin 10 skin which will be discussed in greater detail in the following sections. Dragon Skin 10 has a shore hardness rating of 10 A [7] compared to Ecoflex 00-30's shore hardness of 00-30 [9]. The useful difference between the two is that Dragon Skin 10 has a tensile strength of 475 PSI while Ecoflex 00-30 has a tensile strength of 200 PSI. Having the air chamber portion made out of Dragon Skin allowed a greater force to be applied using higher air pressure without

damaging the actuator. The top sensor continued to be made out of Ecoflex 00-30 because it was found that a Dragon Skin 10 Sensor caused the actuator to extend straight out instead of bending as desired.

At this point in the design, silicone rubber skins were used instead of molded silicone pieces to seal in the sensor and actuator chamber parts. In previous versions the molded silicone pieces would be attached to their corresponding parts by using a wooden applicator to smear a thin layer of uncured silicone between the two. This was woefully ineffective and thus a new solution was needed. Silicone skins created with a spin coater represented a major breakthrough in the manufacturing techniques for this project. To accomplish this an acrylic plate was placed on a spin coater with a dollop of uncured silicone in its center. This was then spin coated at a slow speed to create a thick, even layer of silicone on top of the acrylic. After curing a small amount of uncured silicone was placed on top of the cured "skin". This is then spun coat at high speed and for a long duration to create a very thin layer of uncured silicone on top of the already cured skin. This very thin, very consistent layer served as a glue and allowed the molded sensor and actuator chamber parts to be sealed to the skin without filling in any features or allowing leaks. This change of technique allowed the project to be successfully completed and opened the door to a new range of possibilities in terms of actuator design and feature detail.

One additional minor change was that an enclosed mold was used for this version of the actuator. This was done to make a more even, flat surface along the top chambers of the actuator where the top sensor attached. In previous versions, the open nature of the mold allowed a meniscus effect to take place along certain sections

of the top of the mold. This led to an uneven surface. The molds for this version can be viewed in figure 2.7.

2.4 Actuator Mount Design

Initial designs for a mount had to be redesigned after it was found that having wires only held on by being inserted into the actuators led to the wires being pulled out or snapped off due repeated stress. The final mount design shown in figure 2.10 is composed of 4 pieces and is designed to use bolts to clamp it down onto the actuator. It also features specific holes drilled in to to allow zip ties to be used as strain relief. The sensor wires make a loop around the zip ties before being inserted into the sensor fluid reservoirs. The final improvement is that to prevent the wires and the air supplying needle from being pulled out, the mount is designed to be filled with uncured silicon behind the actuator to fully lock in the components.

2.5 Final Build Procedures

The build procedure was created using trial and error and from taking inspiration from other researchers [17]. It eventually evolved into a multistep process which is listed below.

2.5.1 V1 Construction Steps

1. Mix about 20 grams of Dragonskin 10 Part A [7] with 20 Grams of Part B. Add in 1 gram of Smooth On's Slo Jo [22] and 4 grams of Smooth On's Silicon

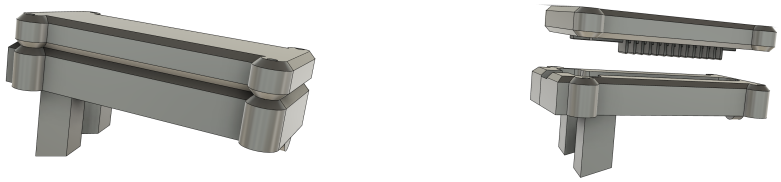

(a) (b)

Figure 2.7: The left figure (A) shows the final actuator chamber mold when the two pieces are clamped together. The Right figure (B) shows the actuator chamber mold when the two pieces are apart. The legs on the mold were put in place to provide tilt to the mold when it was degassing. It was eventually found that it was much simpler and more effective to place it on it's end.

Thinner [21]. The Slo Jo will help to increase the pot life of the uncured silicone and allow enough time to degas the silicone. The silicone thinner will make degassing substantially easier.

2. Make sure the uncured silicone is effectively degassed either using either a vacuum chamber or a degassing mixer system. Pour the Dragonskin 10 mixture into both the actuator chamber molds and the the bottom sensor mold first making sure that the actuator chamber mold is effectively clamped together. These molds can be seen in figures 2.7 and 2.8. Place these in a vacuum chamber to degas making sure to reserve the leftover Dragon Skin 10 mixture.

3. While the Dragon Skin 10 parts are degassing, which can take up to 20 minutes, the Ecoflex 00-30 parts can be made. On the final version of the actuator, only the top sensor is made of Ecoflex 00-30. Mix together 10 grams of Ecoflex 00-

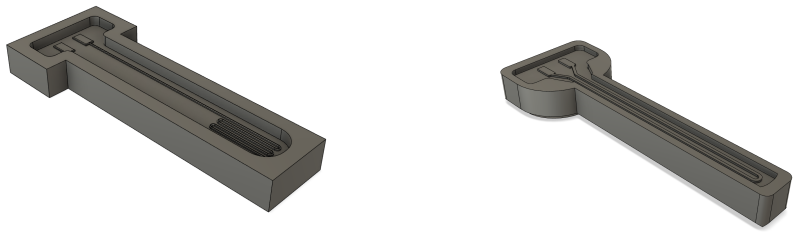

(a) (b)

Figure 2.8: The left figure (A) shows the final version of the Bottom sensor mold, this mold was carried over from Version 2 and was filled with Dragon Skin 10. The Right figure (B) shows the top sensor mold, it was filled with Ecoflex 00-30.

30 Part A and 10 grams of Part B [9]. Ecoflex does not need any mold thinner because of its lower viscosity. Pour the Ecoflex mixture into the top sensor mold, shown in figure 2.8, and place in a vacuum chamber to degas.

4. Once bubbles have stopped coming out of any of the molds, take them out of the vacuum chamber. Top off any lost uncured silicone so that it is level with the top of the mold. For the top and bottom sensor molds, take a piece of acrylic that is slightly bigger than the mold itself and gently lay it down on top of the mold going from back to front. This will serve as a lid for the molds and help to create a very smooth top surface for the top and bottom sensor. When all molds have finished degassing, place them in a $60°c$ oven for about 4 hours to fully cure.

5. While the sensor and actuator chamber parts are curing, the silicone "skins" can be made. Two total skins will be needed for one actuator, one of Ecoflex

Figure 2.9: **This figure shows multiple actuator pieces being glued to a silicone "skin". Once cured they will be cut out of the skin and can then be attached to other pieces to form a complete actuator.**

00-30 and one of Dragon Skin 10 Combine 15 grams each of Dragon Skin 10 A and B ([7]), add 2 grams of of mold thinner [21]. Mix thoroughly and degas. In parallel mix 15 grams each of Ecoflex 00-30 A and B [9]. No thinner will be necessary for the Ecoflex as the viscosity of it unaltered is similar to that of the Dragonskin with thinner. Once both are mixed and degassed, they can be spun coat onto acrylic plates. An image of these plates can be seen in figure A.9. To do this take either the Dragon skin or Ecoflex mixtures and deposit them in the middle of the acrylic plate. Then spin the plate at 100 rpm for 70 seconds. This should create a smooth, even layer. Repeat this step with the remaining uncured silicone and plate. This should result in 2 plates of uncured silicone, one composed of Dragon Skin and One composed of Ecoflex.

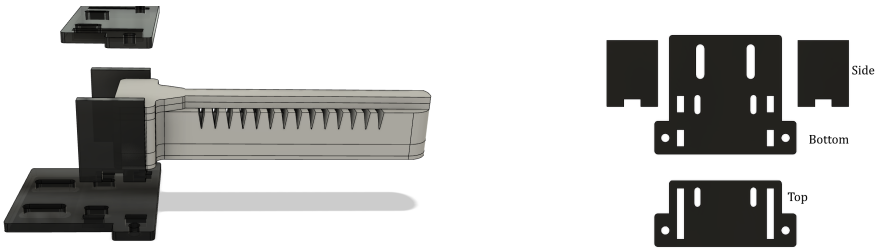

(a) (b)

Figure 2.10: The left figure (A) shows an exploded version of the mount around version 3 while the right figure (B) shows the same mount but flat for ease of viewing.

These can be put to cure in a $60°c$ oven. They can be used in an hour.

6. Once everything is cured, the final assembly of the individual components can be constructed. More uncured silicone will be needed. The same procedures as above can be followed but only a total of 15 grams each of the Dragon Skin mixture and the Ecoflex mixture will be needed. Once these are mixed and degassed, the same silicone mixture can be poured into the middle of the acrylic disk that is covered with the silicone skin, making sure to match the uncured silicon with its same cured silicone counter part. These disks can now be spun at 1800 rpm for 60 seconds. This should create a very thin uncured silicone glue on top of the cured silicone "skin". This needs to be done for both the Ecoflex and Dragon Skin "skins".

7. The molded parts can now be glued to their corresponding "skin". To do this take a molded part and gently lay it down on the uncured silicone glue,

starting at one end of the part and moving toward the other. An image of what this looks like when complete can be seen in figure 2.9. Both the actuator chamber piece and the bottom sensor should be layed onto the Dragon Skin 10 "skin" and the top sensor piece should be put on the Ecoflex "skin". Also shown in figure 2.9 is that when making multiple actuators, usually at least 3 pieces can be fit onto a 5 inch skin. These should be left cure at room temperature. Curing them in an oven can lead to the microscopic air bubbles, caught between the part and the skin, expanding due to heat and affecting the integrity of the seal.

8. After 2 hours the parts should be sufficiently glued to their respective "skins". The parts and the "Skin" that they are glued to should now be cut out of the main skin using a knife. At this point each part should be individually functional and only needs to be combined with the other parts. A visual check of all of the sensor and air channels should be performed. If any look filled in, that part shouldn't be used. If any don't look well attached then a a needle containing uncured Ecoflex 00-30 can be inserted into the part where the two pieces were not glued together effectively. Injecting the silicone can be used to spot fix small problems.

9. To attach the bottom sensor to the actuator chambers, 20 grams of mixed and degassed Dragonskin 10 is spread onto the top of the bottom sensor using a wooden applicator. The actuator part is then gently placed on top and prevented from sliding out of alignment from the sensor using wooden sticks

that are pressed into the surface that the parts are stacked on. Everything is then placed into the vacuum chamber to try and remove all air bubbles between the bottom sensor and the actuator. After the air bubbles have stopped coming out this can be put in the oven to cure for two hours.

10. At this point the top sensor needs to be attached to the combined actuator and bottom sensor. Issues were found when using a wooden applicator to apply uncured resin to the top sensor. Uncured resin would usually drip down and cure on top of the actuator chambers causing an uneven expansion of the chambers. To prevent this the following procedure was developed. An acrylic plate with a cutout that exactly matches the top sensor is attached to one of the acrylic disks using double sided tape. This acrylic plate can be seen in figure A.9. The top sensor is then gently placed inside of the cutout and then the whole apparatus is placed on the spin coater. A bead of uncured Ecoflex 00-30 is put down the length of the top sensor. Run the spin coater for 1 minute at 70 rpm. This should apply an even layer of uncured Ecoflex on the whole top sensor. Then with the top sensor still inside of the acrylic cutout, place the assembled actuator and bottom sensor topside down on the top sensor. This can then be placed in an oven to cure for 2 hours. Doing this should complete the actual construction of the whole actuator but does not include adding the sensor fluid and mounting the actuator.

11. To flood the sensor channels with the ionic fluid 1-Ethyl-3-methylimidazolium ethyl sulfate (1E3MES) [20], two syringes need to be prepared. One contains

1E3MES and another contain uncured Ecoflex 00-30 [9]. The sensor fluid described in this paper also usually had some amount of food dye mixed in to make the sensor ink, which was normally translucent, more visible. This had the added benefit of make leaks much easier to detect during development. The following instructions are applicable for both the top sensor and the bottom sensor. The first step to flooding a sensor is to place a hollow needle into one of the sensor reservoirs, which allows the air to escape when the sensor fluid is injected. Using the needle filled with 1E3MES, carefully inject the sensor fluid into the fluid reservoir opposite the one containing the hollow needle. The fluid should slowly fill the entire length of the sensor channel. Continue until the sensor fluid comes out of the hollow needle. Make sure to remove all air bubbles with an empty needle and then remove both the 1E3MES syringe and the hollow needle. The sensor channel should now be filled with sensor fluid. It will seem like it will stay in the channel on it's own but over time it will leak out unless it is sealed in properly.

To seal off the sensor channels, a silicone cap is placed inside of the sensor fluid reservoirs. After completely filling the sensor channels with fluid and removing all air bubbles, take the syringe filled with uncured Ecoflex 00-30 and inject some of it into the end of the sensor fluid reservoir which is where the needle that had filled the sensor pierced through the silicone. Inject enough that about half of the reservoir is filled with Ecoflex 00-30 and half is filled with sensor fluid. Allow this to cure at room temperature for 2 hours.

12. After the above, the actuator still need to be mounted and electrically wired. The mount was made using laser cut acrylic pieces. It features holes to allow a bolt to clamp the actuator, slots to allow zip ties to provide strain relief to the sensor wires, and finally a set of slots in the back of the bottom part of the mount that would allow it to be bolted onto a structure. Install the mount as shown in figure 2.10, inserting two long M3 bolts through the two holes on the tabs on both the top and bottom pieces. This serves to effectively clamp the actuator in the mount. Next loop two zip ties through the holes directly behind the actuator, these will be used for strain relief. Take 4, 24 gauge, solid core sensor wires, about 3 foot long each and wrap them around the zip ties before finally poking one into each separate sensor fluid reservoir. Insert a large gauge needle into the back of the actuator's air channel.

13. If not resealed, the new holes created by the wire will allow the sensor fluid to leak out of the actuator. To circumvent this, the mount has been designed to form a box around the end of the actuator, allowing uncured elastomer to pool and cure there. The final step is then to place the actuator vertically in an oven with the mount on as well. Then pour uncured Ecoflex 00-30 ([9]) into the end of the mount. Reserve some of the ecoflex outside of the oven to pour in incrementally due to elastomer leaking out of the mount.

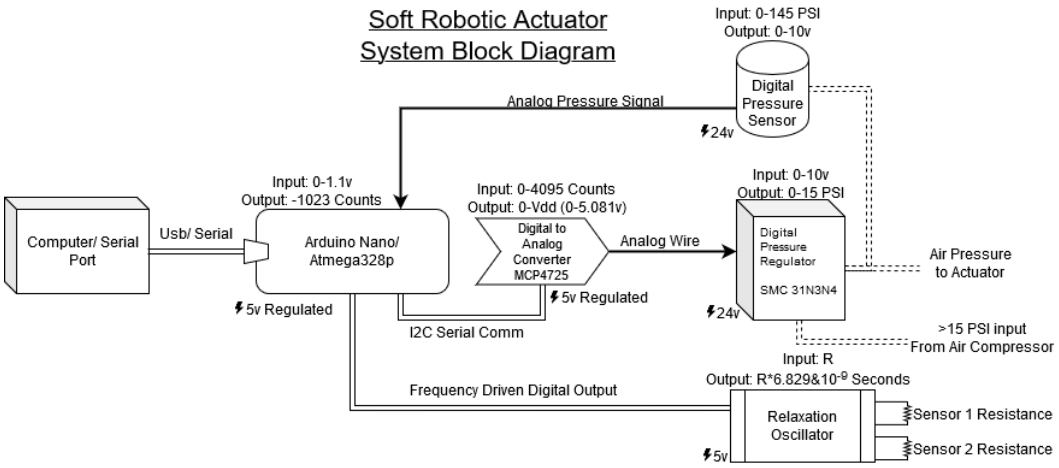

Figure 2.11: This figure shows the complete system setup need to collect data from one of the actuators. The central component of the system is the Arduino Nano which was used for both controlling the actuator and for taking data in from it's sensors. This data was then sent via serial port to the computer.

2.6 Electrical System

The total system required to control and sense the actuator has quite a few individual pieces. These components can be seen in total in figure 2.11. The list below details the function of each individual component.

- Arduino Nano, Atmega328p [1] - The Arduino Nano is a low cost 8 bit Microcontroller that is coded using Arduino's custom Integrated Development Environment and coding language which is similar to C++. It was chosen due to its low cost, small size, and ease of programming. It can be powered by the computer it is connected to but for an accurate ADC reading, it should be provided a low noise, consistent 5v signal.

- Digital to Analog Converter, MCP4725 [15]- This DAC is made by Microchip and was crucial to controlling the pressure regulator which could only take in an analog signal. It being a full range DAC with 12 bit precision could control the pressure regulator up to slightly over 7.5 PSI. It is powered by the same regulated 5v as the Arduino Nano.

- Digital Pressure Sensor, Balluff BSP000W [3]- The pressure sensor was chosen based on it's high accuracy and the fact that it has a 0-10v output, proportional to 0-145 psi. The pressure sensor is powered of of a 24v DC wall adapter.

- Digital Pressure Regulator, SMC ITV2030 [23]- This pressure regulator provides a regulated pressure that is set by a 0-10v input, It requires an air source that has a pressure greater than 15 PSI. It runs off of the same 24v as the pressure sensor.

- Relaxation Oscillator Circuit - The relaxation oscillator circuit is a custom inhouse PCB that was designed to measure the impedance of the sensor fluid in the actuator without hydrolizing the sensor fluid. It measures the impedance of both the top and bottom sensors and converts that to frequency through a relaxation oscillator.

The central component of the system is the Arduino Nano, which serves to both collect data and relay it to the computer while also running a feedback loop to control the position of the finger. It was connected to the computer using a USB serial communications port through which it sent data including time, input pressure, observed pressure, and the actuator sensor values. Without an onboard digital to

analog converter, an offboard one was provided. This DAC was used to control the Digital Pressure Regulator which can take in $0 - 10v$ and turns that into 0-15psi. Due to the fact that the DAC can only go up to just over 5v in output, the actuator could only be pressurized to 7.5psi which was sufficient. The digital pressure sensor output an analog signal proportional to the input pressure, this was then sampled by the arduino. The relaxation Oscillator was used to sample the impedance of the top and bottom sensor. This is described in greater detail below, the relaxation oscillator outputs a variable frequency depending on the sensed impedance. This was sampled by the arduino using an interrupt and a timer to get the period of the signal.

2.6.1 Relaxation Oscillator

A relaxation oscillator was used to turn the variable impedance of the top and bottom sensors into a readable square wave signal. This was done because more conventional methods of measuring impedance would not work for this system. The usual method would be to apply a known DC voltage to to a known resistor in series with the sensor and then measure the voltage where they meet as a form of voltage divider. This would not work for the sensor because the ionic fluid, 1E3MES [20], will break down due to electrolysis when presented with a high voltage, DC signal [4]. To work around this, the relaxation oscillator was used which will oscillate between $+0.16v$ and $-0.16v$ across the sensor while still producing a very readable $0v$ to $5v$ signal. A relaxation oscillator is a good choice because it has be used before [28] with 1E3MES and because it plays well to one of the strengths of a microcontroller

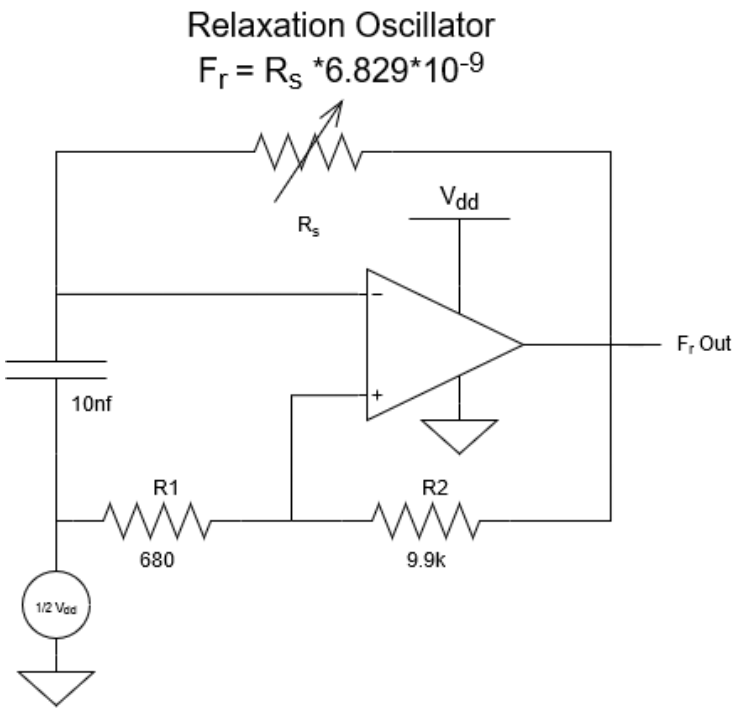

Figure 2.12: **The above figure shows the relaxation oscillator circuit used to measure the impedance of the sensor fluid. The relaxation oscillator uses Resistor Capacitor charge time constant to output a variable frequency square wave based on the sensor resistance.**

which is precise measurement of timing. The schematic for this circuit can be seen in figure 2.12. To determine the impedance of the sensor the following series of equations can be used to calculate the output frequency (f_s) relative to the sensor R_s or the output period (P_s) relative to the sensor.

$$k = \frac{R1}{R1 + R2} \tag{2.1}$$

$$k = \frac{680}{680 + 9900} \tag{2.2}$$

$$k = 0.0642 \tag{2.3}$$

$$f_s = \frac{1}{2 * R_s * C * \ln \frac{1+k}{1-k}} \tag{2.4}$$

$$f_s = \frac{1}{2 * R_s * (10 * 10^{-9}) * \ln \frac{1+0.0642}{1-0.0642}} \tag{2.5}$$

$$f_s = \frac{1}{R_s * (2.57 * 10^{-9})} \tag{2.6}$$

$$f_s * R_s = \frac{1}{(2.57 * 10^{-9})} \tag{2.7}$$

$$R_s = \frac{3.891 * 10^8}{f_s} \tag{2.8}$$

$$R_s = P_s * 3.891 * 10^8 \tag{2.9}$$

The above equations take values from the schematic shown in figure 2.12, showing that there is a clear conversion impedance R_s to period and or frequency . The use of a relaxation oscillator to measure impedance has one very distinct advantage. The capacitor C is the key determinant, besides R_s, in determining the output frequency of the oscillator. As such increasing the size of the capacitor could would make the output a lower frequency with a longer period and a smaller capacitor would make a much higher frequency. This could be used strategically to affect the overall performance of the sensors. As the capacitor is charging in real or "analog" time it is in a sense finding the average impedance of the sensor over that time span. Consequently it can be assumed that if low noise, accurate measurements are required then making the capacitor larger would a net positive outcome on the

system. By the same logic, if a very fast moving control loop was required then the capacitor should be made smaller at the expense of the accuracy, noise, and overall resolution.

To enable consistency across measurements and reduce errors, this circuit shown in figure 2.12 was made into a PCB. The pcb featured an onboard 5v linear regulator to reduce noise. It was also designed to handle two sensor signals using two separate relaxation oscillators. This allowed it to provide data for both the top and bottom sensors of any given actuator. In addition the entire circuit as seen in figure 2.12 was offset by 2.5v, this allowed the use of a single output powersupply without compromising the integrity of the sensor fluid. The schematic and pcb as described above can be seen in figures A.10 and A.11 in the appendix.

Chapter 3

Design Verification

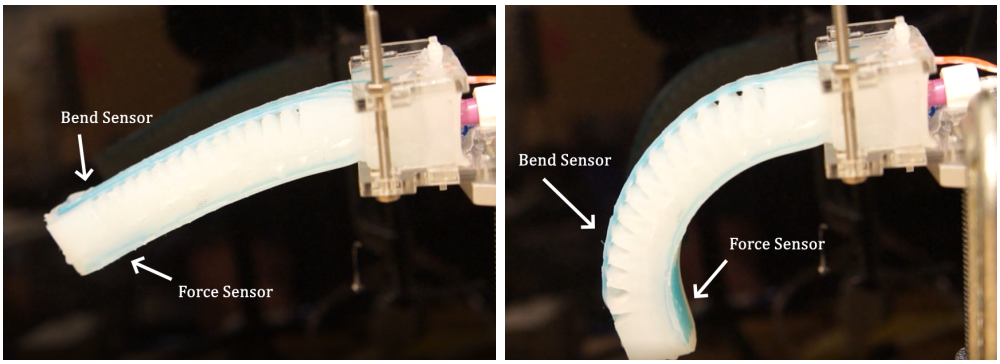

(a) (b)

Figure 3.1: These figures show the actuator mounted in free space so that it cannot encounter any obstacles when being inflated.

Just as important as designing the actuators and implementing a construction methodology for them is showing that the total system is valid and useful. This section will show what experiments were performed to observe the responsiveness of both the top and bottom sensors concerning air pressure and external objects. These tests were necessary before implementing the control algorithm because they

provided confidence in the design.

3.1 Sensor Characterization

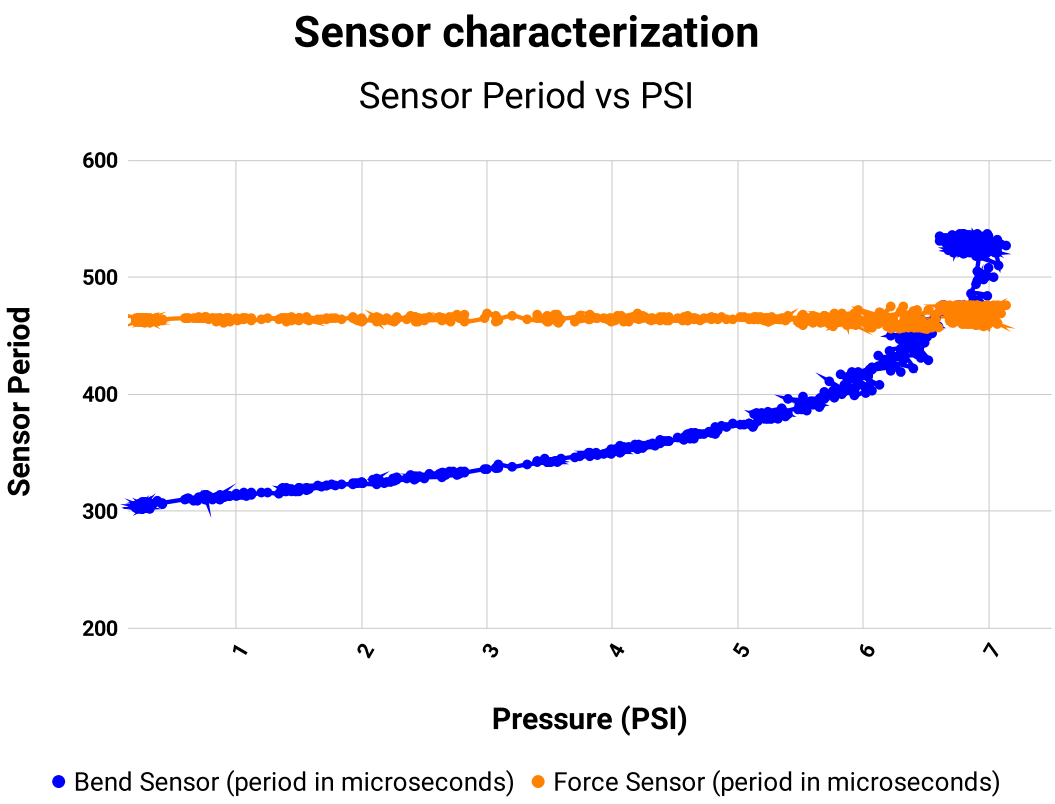

Figure 3.2: This figure shows the characterization of the actuator's sensors verses input pressure.

The first step in verifying the validity of the sensor design was to characterize the bend sensor's response to input pressure. Characterization served two purposes: (1) demonstrate a basic level of effectiveness in bend sensing and (2) generate an equation representing the relationship between input pressure and bend sensor output. Such characterization can then be utilized to create a feedback control loop,

as shown in chapter 5.

The setup for this test required minimal complexity; the actuator was mounted horizontally on a stand at such a point that when inflated, it would not brush against any objects that might affect its bend. Utilizing the testing rig enabled the actuator to be tested in a controlled environment with minimal pressure, as shown in figure 3.1. The passive tilt of the actuator from the effects of gravity is primarily due to the actuator's nonrigid nature. However, the mounting system's flexibility also contributes. The system required only some of the components, as shown in figure 2.11. A relaxation oscillator is used to obtain sensor data, which is recorded by the Arduino microcontroller. The Arduino also measures system pressure, but instead of being supplied by the digital regulator, it adheres to an analog regulator. An analog regulator was chosen in place of a digital component as an analog regulator would have a more continuous transition between various pressures. Thus, analog provides a better data set for characterizing the sensor. Also, as noted in the following sections, the digital regulator adds a fair amount of oscillatory noise to the system as its valves open and close. Therefore, the noise of a digital regulator lessens the quality of the sensor data.

In performing the test, pressure for the analog regulator was started at 0 psi and very slowly increased to 7 psi. Once seven psi was reached, the pressure was slowly released. This whole task was performed slowly to try to maximize the number of data points that were captured. Seven psi was chosen to avoid overstressing the actuator; previous actuators had been shown to take pressure up to 9 psi but much past that, and they could have a malfunction and be irreversibly damaged.

The response from the bend sensor test demonstrates a quantifiable curve while the force sensor is relatively flat, as seen in figure 3.2. Such results are a desired response for actuator control. It should be noted that variation in the force sensor signal does appear to get more significant at higher PSI's, greater than 5.5 PSI. This variation is most likely due to the vibrations that result from the actuator changing shape in free space; it will be shown in a later section that this has little bearing on the force sensor when it comes in contact with an actual object. The bend sensor has some variation in output data; it was noticed that increasing pressure seems to be slight offset from the data when decreasing. This could be due to a few factors, one being that the pressure sensor was not located directly next to the actuator and thus could have been recording a slightly different pressure than the actuator, especially as pressure is being released. This could have also been caused by the actuator taking time to settle as the pressure decreased due to the only source of backpressure being the actuator itself. While these issues could have an impact on the actuator's very fine control, with the crudeness of the digital pressure regulator in the following section, it is not a big issue. The data was used to characterize the bend sensor into a 4th order polynomial. This is shown below, where p represents the input pressure, and T represents the period in microseconds.

$$T = 0.46p^4 - 3.1p^3 + 7.2p^2 + 12p + 420 \tag{3.1}$$

This polynomial would be crucial in controlling the bend angle of the actuator in chapter 5.

3.2 Square Wave Input

As seen in the previous section, the actuator did experience some delay in reaching a set bend due to input pressure. This was noted by observation during the previous characterization tests. There is also some delay induced by the digital regulator which functioned by opening and quickly closing a valve to let in air from a high pressure source. The following tests were performed to better understand how these delays might affect the responsiveness of the actuator. These tests consisted of giving the actuator a square wave pressure input that would switch between low and high pressure every 5 seconds. Just like the characterization test, the actuator was suspended in free space and the pressure was recorded. The digital pressure regulator controlled the pressure. Only the bend sensor data is relevant for this test because from the previous test it was shown that the force sensor had little to no response due to pressure when suspended in free space. Two separate tests were performed to get a better idea of how the actuator responds to changes in pressure and and responds to the noise from the digital regulator. The first test oscillated between 0 and 6.5 PSI, which corresponds to the lowest and the highest pressures that the actuator would encounter. The second test was from 1 to 5 PSI. This was done to determine what falling to a lower pressure would do if that pressure was still higher than atmospheric.

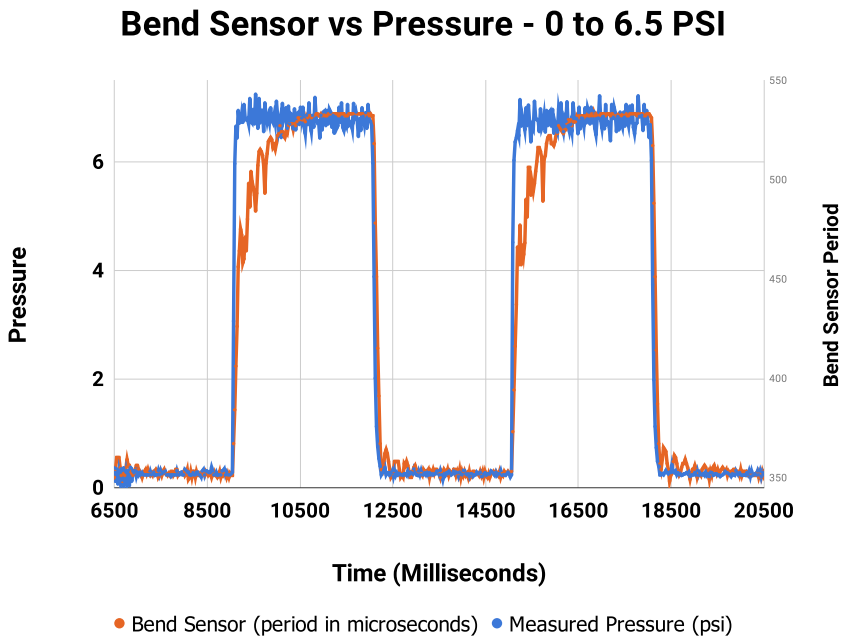

Figure 3.3: **This figure shows the bend sensor's response 0 to 6.5 PSI square wave as compared to the measured system pressure.**

3.2.1 0.0 to 6.5 PSI Tests

The first test required the actuator to have an alternating pressure applied to it from 0 to 6.5 PSI. The pressure would take a total of 6 seconds to cycle, spending 3 seconds at 0 PSI and 3 seconds at 6.5 PSI. The goal was to observe and plot the bend sensor and the system pressure as a result from a given a step input by the digital pressure regulator. The results from this experiment can be seen in figures 3.3 and 3.4. Figure 3.3 shows how this was performed by setting the pressures at either 0 or 6.5PSI. The blue line represents the measured pressure, which rose reasonably quickly to its set value but had quite a bit of variability, seeming to alternate from 6.5 to 6.8 PSI. The data readout from the bend sensor rose much more slowly and seems to have taken almost 2 seconds to reach it is steady-state value. By observation,

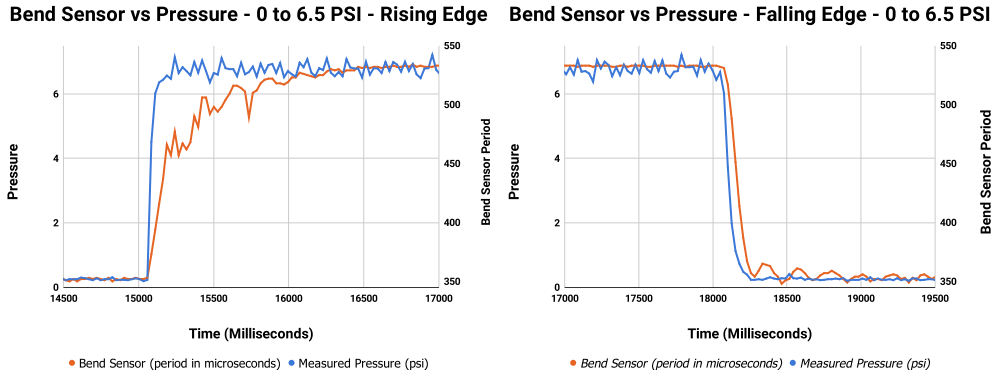

(a) (b)

Figure 3.4: These figures are a close up of the square wave's rising and falling edges as shown in figure 3.3

the sensor was accurately reflecting the motion of the actuator. This data is also reflected in figure 3.4, which shows a closeup look of the rising edge at 9 seconds. This figure further reinforces the fact that the actuator lagged behind the input pressure. The other part of figure 3.4 shows the falling edge as the pressure shifted from 6.5 to 0 PSI. Once again, the actuator lagged behind the pressure. However, the settling time seems faster than when it rose to 6.5 PSI. This may be due to the controller's lack of vibration because the controller was fully open to atmospheric pressure in this setting. This is reinforced by the fact that the pressure plot of the falling edge has almost no noise as compared to the rising edge. This test, while informative, seemed to have been affected by by the extremely low and high pressures. The 0 psi input caused the pressure regulator to turn fully off, reducing system noise while the high-pressure input took some time to arrive at a steady-state value. Consequently, a follow-up test was performed, where the actuator oscillated

between 1.0 and 5.0 PSI every 3 seconds.

3.2.2 1.0 to 5.0 PSI Tests

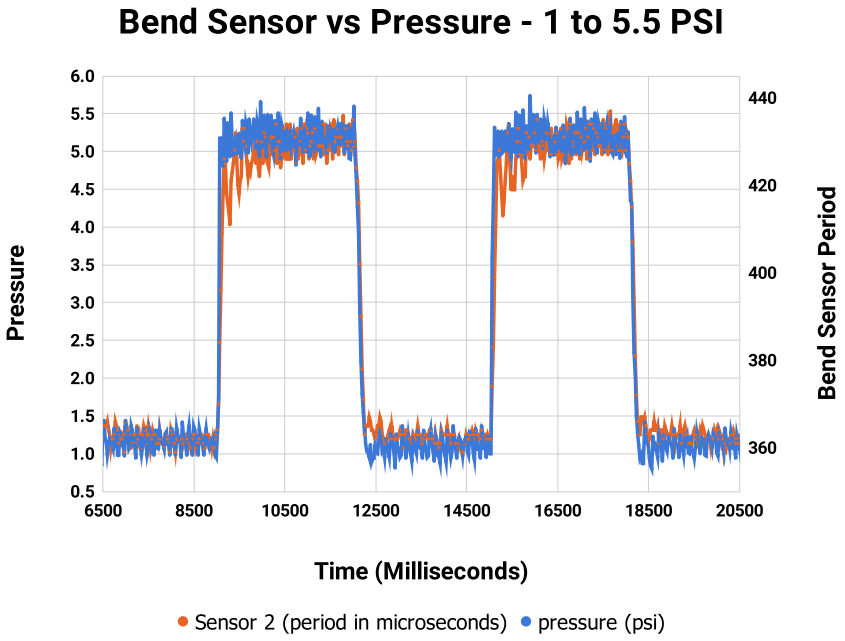

Figure 3.5: This figure shows the bend sensor's response 1 to 5 PSI square wave input as compared to the measured system pressure.

The results of this test are shown in figures 3.5 and 3.6. This test was conducted in the same way as the previous with pressure alternating between 1.0 and 5.0 PSI every 3 seconds. What is interesting is the response to high pressure, and low pressure is noticeably different. In figure 3.4, it can be seen that the lag between the pressure changing and the actuator responding is much smaller than the previous test. Noticeable on the rising edge plot is that the actuator still takes some time to settle after encountering 5.5 PSI. The falling edge graph is interesting because before the pressure goes down to 1.5 PSI, the readouts from the bend sensor seem to match

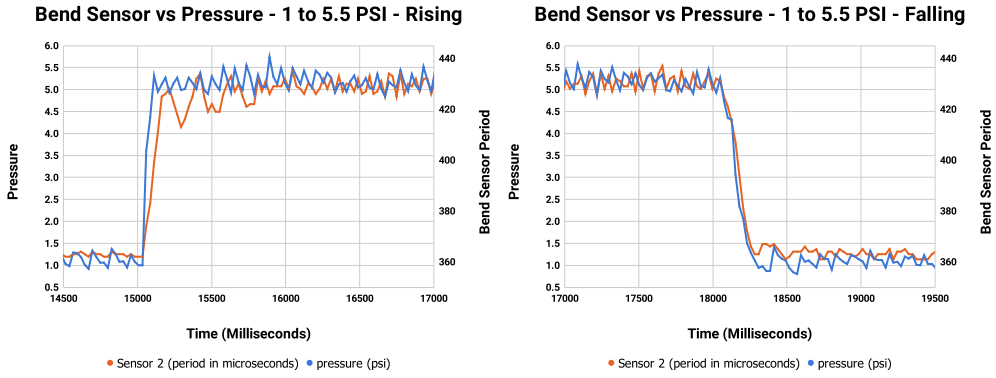

(a) (b)

Figure 3.6: These figures are a close up of the square wave's rising and falling edges as shown in figure 3.5

the pressure sensor's noise in terms of frequency. This seems more pronounced than the noise on the 6.5 PSI graph in figure 3.4. This is partially due to the scale difference between figures 3.4 and 3.6, but it is also is probably due to the pressure that the actuator was set to. The lower pressure means that the actuator is under less stress. Thus minor changes in pressure can cause more significant swings in the equilibrium between the air and the stretched silicone. Interestingly both going up to 5 PSI and going down to 1 PSI followed the PSI graph more closely, probably due to the shorter distance between PSI values.

Both tests were informative, and both clearly showed that the digital pressure regulator is noisy enough to affect the actuator, which the bend sensor was precise enough to measure. Another thing of note is that the system smoothly goes up to a set pressure, but falling to a lower pressure takes longer, reflected in both the PSI measurements and the bend sensor. The digital regulator has 15 psi attached to

it, which has enough potential energy to easily get the actuator up to the desired pressure quickly and efficiently. However, the air outlet for the digital regulator opens up to atmospheric pressure. Thus, the stretched actuator's potential energy is the only influencer that can force air out of the system. In terms of system improvements, using bigger tubes and needles could reduce the delay between the actuator and the pressure input. Overall the actuator seems responsive enough to changes in air pressure, and the bend sensor has a high enough sample rate to measure the changes in bend when transitioning between pressures.

3.3 Force Tests

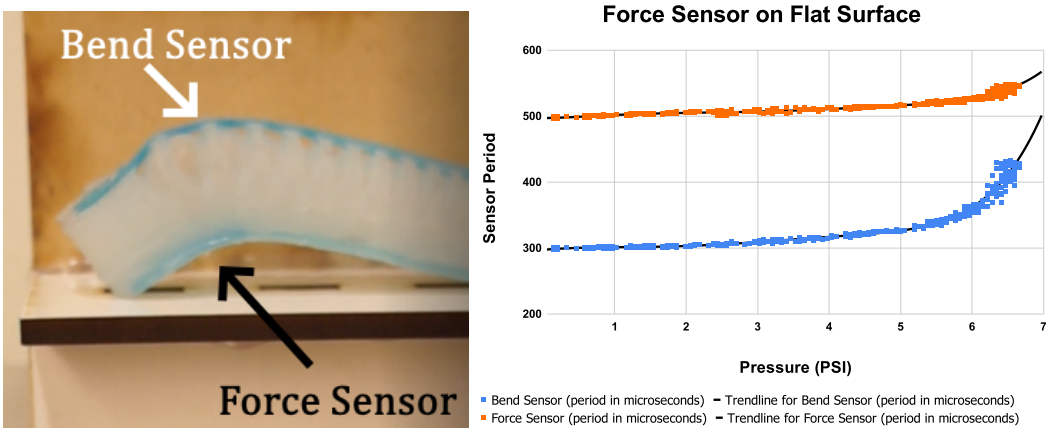

(a) (b)

Figure 3.7: This figure shows the setup for the initial force test and the result of that test in which the actuator was pressurized while in contact with a flat object.

With the previous tests demonstrating the effectiveness of the bend sensor, the

force sensor also had to be explored. The previous tests were conducted in free space, which should have little to no effect on the force sensor. The following tests were performed with the actuator in contact with an object. Only one test was initially planned, but due to the poor results, other tests were executed as well. All of the tests were conducted in the same way; the actuator was mounted so that it rested on an object, and then the actuator was pressurized up to 6.5 PSI using an analog regulator. The pressure was then slowly released. The top bend sensor and the bottom force sensor were recorded, but only the force sensor data is useful for these tests.

The first test consisted of placing the actuator in contact with a flat surface, this setup, and the results are shown in figure 3.7. The actuator tends to lift when on a flat surface due to how the actuator was designed and. It tends to bend around obstacles rather than applying force to it because this the path of least resistance for the air pressure. The force is still being applied but only at the very tip of the actuator where no parts of the force sensor are located, as shown in figure A.1. This is reflected in the sensor output, which only changed from 500 microseconds to 540 microseconds with respect to 0 and 6.5 PSI. While this test was informative, it did not adequately display the usefulness of the sensor. As a result, the following tests were performed in which the actuator was inflated when in contact with both a post and a cylinder.

The next test was performed with the actuator in contact with a post. This is shown in figure 3.8. The post was chosen because it would allow the actuator to apply force over a much smaller area, which should increase sensor response. The

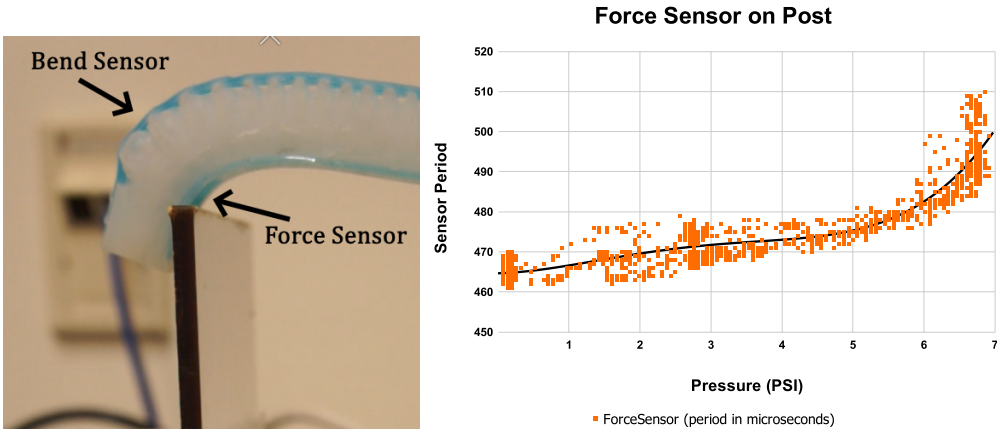

(a) (b)

Figure 3.8: These figures show the setup for the second force test in which the actuator was pressurized while the force sensor was in contact with a post.

post was placed so that in its a relaxed state, the actuator's force sensor was centered on the post. The picture shows that the actuator's tendency is still to bend around the obstacle, but the post is still remains in contact with the force sensor. The graph tells a similar story: the force sensor clearly has a more significant response than the previous test on the flat surface. The response is also reasonably linear up until around 6.3 PSI. At 6.3 PSI, the force sensor's output increases, and the general response is significantly different from the lower PSI values. This is probably due to the sensor channels being pinched off by the post, which would significantly increase the impedance of the sensor. To confirm these results, an additional test was performed in which the actuator was pressurized against a cylinder instead of a post.

The final test had the pressurized actuator placed against a cylinder, as shown

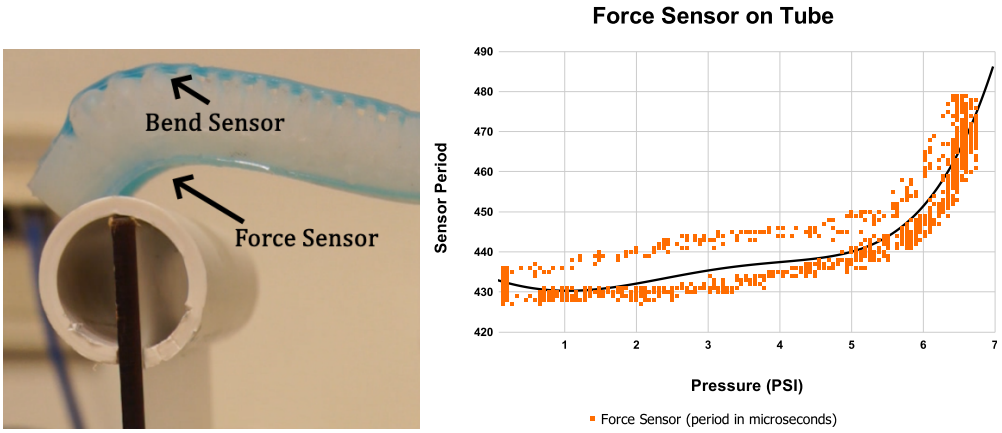

(a) (b)

Figure 3.9: **These figures show the third force test in which the actuator was pressurized while in contact with a tube.**

in figure 3.9. This test was performed in the same way as the previous tests and had the cylinder centered under the force sensor. Overall the results were similar to the force test on the post but with a few minor differences. In this test, the transition from the mostly linear low force response to a high force response is more gradual. This response is probably due to the round shape of the cylinder. This reinforces the observations from the previous test, which showed that some point, the force begins to severely pinch off the sensor channels, significantly increasing the impedance. Overall all of these tests do show that the force sensor is responsive and has potential applications to assist the actuator with gripping objects.

3.4 Conclusions on Design Verification Results

The initial characterization tests gave a practical demonstration of the bend sensor and allowed an equation to be found representing the bend sensor's response to pressure in free space. This allows for the control system discussed in the following chapter. The square input tests were useful for showing the limitation of the system in tracking input pressure. This leads to the conclusion that in future system iterations, the needle size may have to be increased to allow more air into the actuator. However, in the current system, it is an additional factor to account for when considering the controllability of the robot. Finally, the force tests were effective at demonstrating the responsiveness of the force sensor. When the force sensor was actually in contact with an obstacle, as shown in figure 3.8 and 3.9, the sensor is relatively responsive. However, it does seem to have a point where the response changes significantly. This is something that needs to be accounted for but could be an advantage. If the response of the force sensor was thought of as somewhat binary, the sensor's sudden change in response due to increased force could determine if the gripper has a reliable hold on an object. This could be a simple solution to trying to map the force sensor's response to pressure being that only a known force threshold would be required to make the force sensor useful.

Chapter 4

Design Implementation

As discussed in the background section, the next step in the evolution of soft robotics is controllability. This will allow soft robots to actualize their potential and open a wealth of potential applications. As such to fully prove the viability of the design presented in this thesis it stands that it must be used with a feedback control loop. A controller was designed using techniques discussed in a "Movement Error Based Control for a Firm Touch of a Soft Somatosensitive Actuator" [2]. This paper sought to design a controller that could transition between tracking a curvature reference signal to tracking a force reference signal when coming in contact with an object. This would be accomplished by placing the bend and force sensors in a feedback loop. It would be given a ramp signal for the bend sensor to match and when the error becomes too great between the ramp and the bend sensor due to coming in contact with an object, the system would automatically switch to tracking the force sensor in an effort to maintain contact with the object. For the purposes of this demonstration, only the ability to track a ramp signal was

tested. The controller was designed as a simple 2nd order linear controller which was found in part using the characteristic equation that was found in chapter 3.1 which mapped input pressure to bend sensor response. The setup for this system is the same as the square input tests in chapter 3.2. The actuator was suspended in free space and input pressure was controlled by the digital regulator while the bend sensor combined with the relaxation oscillator was used to close the control loop. Two tests were performed, the first in which the controller was applied to a reference ramp signal that was well within the normal operating range of the actuator. The second test was given a reference ramp that exceeded the normal operating range of the actuator.

4.1 Normal Range Control Test

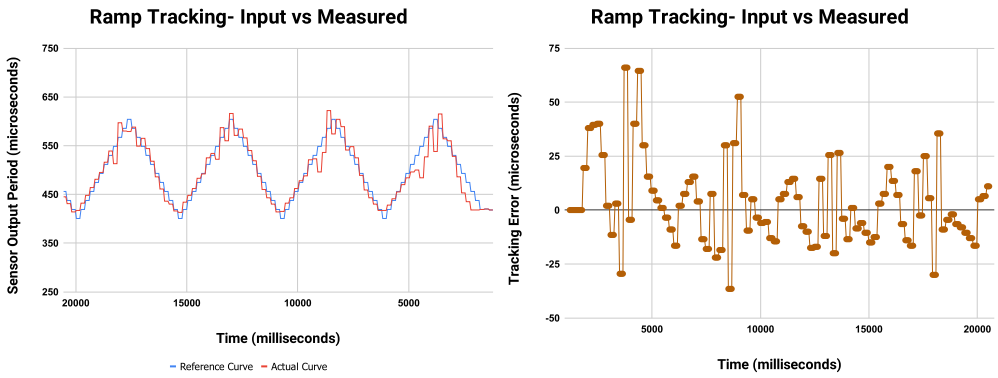

(a) (b)

Figure 4.1: The left Figure (a) shows the actuator tracking a ramp input while the right figure (b) shows the error from this tracking.

The results of the first control test are shown in figure 4.1. For this test the

reference ramp's parameters were chosen so that they stayed well within the normal operating parameters of the actuator. Specifically the pressure limits of 0 to 6.5 PSI. The higher pressure, 6.5 PSI, was chosen to increase the longevity of the actuator and prevent overstressing of the silicone. The results of this test was fairly successful. The actuator, as can be seen in figure 4.1 (a), managed to closely follow the ramp with only a slight delay and the occasional over or undershoot. This is quite good being that the actuator in free space behaves much like a spring and is prone to vibration and has little inherent dampening. The error from this test can be seen in part (b) of the same figure. Overall the error is minimal with most recorded data points being under ± 25 microseconds where microseconds is the recorded period of the signal coming from the relaxation oscillator.

4.2 Unreachable Range Control Test

One final test was performed to verify the effectiveness of the actuator in a control loop. The control loop was given a ramp signal to track that far exceeded the maximum pressure specifications of the actuator. This test was performed to demonstrate that the control loop could successfully recover from a large tracking error value. This could cause excess windup of the control output as error increases. This type of situation could occur if the force part of the controller [2] were ever implemented. The results of this test are shown in figure 4.2. What can be observed is that the actuator successfully tracked the pressure up until a certain point after which the software pressure limiter took over and limited the output pressure to

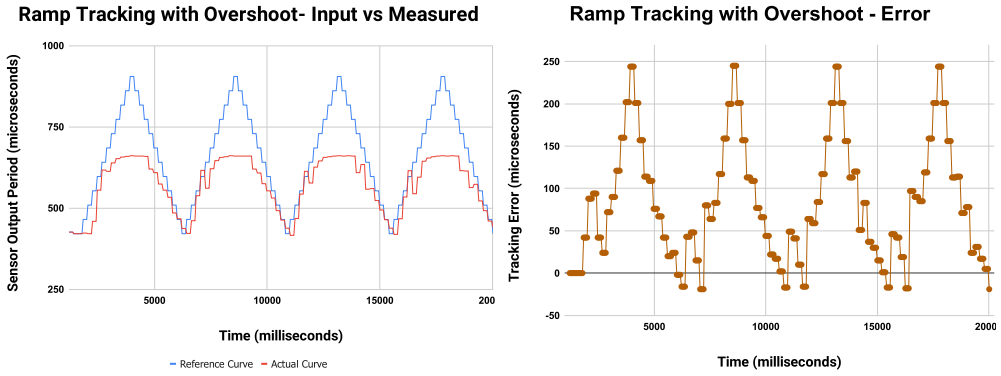

(a) (b)

Figure 4.2: The left Figure (a) shows the actuator tracking a ramp input where the ramps desired curvature value exceeds the maximum allowable pressure for the actuator while the right figure (b) shows the error from this tracking.

prevent damaging the actuator. Once the ramp signal decreased the controller successfully continued to track the reference as it moved back into the working range. This is also reflected in the error value in which the error is much more significant than in figure 4.1 but always returns to zero.

Showing that the total actuator system could be successfully controlled is instrumental to demonstrating the effectiveness of this actuator design. As such the results discussed previously show that the use of an ionic liquid sensor can make an actuator easily controllable.

Chapter 5

Future Design Possibilities

In previous sections it was shown that this project was ultimately successful and opened up the potential for a fully controllable soft robot. This success has also opened up the potential for further explorations and improvements upon this design. There are many possibilities still to explore that could make the actuator even more useful. This section will briefly explore and justify some of those possibilities.

5.1 Improving the Force Response

The actuator's force sensor was shown to be responsive to external objects when the actuator was inflated but as shown in section 3, the overall response of the force sensor to pressure changed dramatically around 5.5 PSI. This was assumed to be due to the force applied to the sensor having overcome the structure of the sensor channels and starting to pinch them. As a consequence, future design improvements should be made to address this issue. The simplest method may be by changing the shape of the sensor channel. At the moment the cross section of a sensor channel

is a rectangle as shown in figure 2.3. This shape could be causing the channel to collapse sideways, similar to crushing a cardboard box. Changing the shape to either a triangular or a half circle could cause the channel to squish in a more uniform matter. The general design of the force sensor could also be changed by making it significantly wider than it is tall. This would distribute force over a larger area and may prevent the channel from totally collapsing as well as increasing the overall responsiveness to small forces. The material that the sensor portion is made out of could also be changed, currently it is made out of Dragon Skin 10 [7] but making it out of a harder material such as Dragon Skin 30 [8] could prevent sensor chambers from collapsing.

5.2 Improving the Actuator's gripping Force

The actuator was found by observation to be able to grip small lightweight objects such as batteries and screwdrivers but was incapable of lifting heavier objects such as containers of uncured silicone or rolls of heavy tape. This supports the assumption that the actuator could be improved to be able to lift and grip heavier objects. This is limited by the resistance of the silicone to overstretching at high pressures. Higher PSI inputs would make the actuator capable of gripping heavier objects. To make this possible the actuator would have to be designed using harder silicone rubbers such as Dragon Skin 30 ([8]).

The overall method by which the actuator bends could be redesigned. Currently the air chambers inside of the actuator inflate like balloons which push against each

other to form a curve. This leads to a continuous stretching of the silicone every inflation which could overstress the actuator and eventually make it unusable. To counteract this future actuators could be designed so that they unfold rather than inflate in an action similar to an accordion. This could allow the actuators to apply more force and use higher pressures without stretching the silicone too much.

5.3 Increasing the Actuator's Biocompatibility

The main ingredients of the actuator, the Dragon Skin 10 [7] and the Ecoflex 00-30 [9] can be considered biocompatible even if not specifically approved for surgical applications. The one hold up with this design and using it for medical applications is that the ionic sensor fluid (1E3MES) is not bio compatible and is even toxic. Thus, finding a more bio compatible sensor fluid would be advantageous in extending the abilities and usefulness of this sensor technology. Inspiration could be taken from other sources [18] to find an alternative. One very promising replacement would be to use a glycol-saline solution. This has the advantage of being both ionic and biocompatible. There is the possibility that water will slowly evaporate out over time but this would not be an issue over the space of a few hours. This fluid should work with the current sensor design, only possibly requiring a change in capacitor value for the relaxation oscillator.

The overall success of this project has opened up many options in terms of future research to explore. In this section a few possible areas of future interest have been outline including improving the force sensor and improving the overall bio

compatibility of the actuator.

Chapter 6

Conclusion

Soft Robotics is still a new and emerging field, but it will need more sophisticated forms of control to unlock its potential as an integral and staying technology. These, in turn, will be driven by capable, intrinsically soft sensors. It was shown that through an iterative design process, a technique was developed to create a soft actuator with integrated bend and force sensors. This consisted of laminating multiple layers together using skins to prevent the uncured glue from filling in features. The actuator was made out of various materials to maximize sensor responsivity relative to overall force output. The actuator was designed in such a way to make construction relatively low cost, requiring minimal equipment. The constructed actuator was shown to have a linear bend sensor output relative to input pressure. It was also shown to be responsive enough to display the digital regulator's effects of electronic pressure control. The actuator was also shown to be responsive to force sensor inputs; however, it was shown to have a sudden change in response around 6 PSI. With the sensors evaluated, it remained to demonstrate that the actuator

could be effectively controlled. Ultimately it managed to track a ramp signal with minimal error using the bend sensor to close the feedback loop. Finally, ideas were presented to allow further improvements on this design and to unlock the potential for more extensive and robust applications.

Appendix A

Additional Design Figures

This section contains additional figures and dimensional drawings from the various versions of the actuator. For the sake of brevity they were excluded from the main document but were included here for thoroughness and to allow repeatability for future researchers. The designs shown here are explained in greater detail in chapter 2.

A.1 Version 1

A.1.1 V1 Design

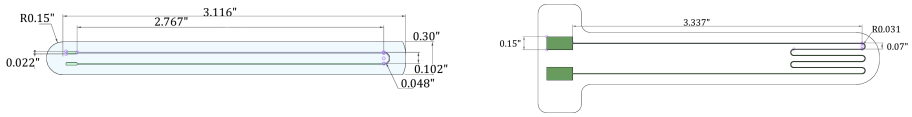

(a) (b)

Figure A.1: **The above figures show the drawings and dimensions for the top and bottom sensors of Version 1 of the actuator.**

A.1.2 V1 Molds

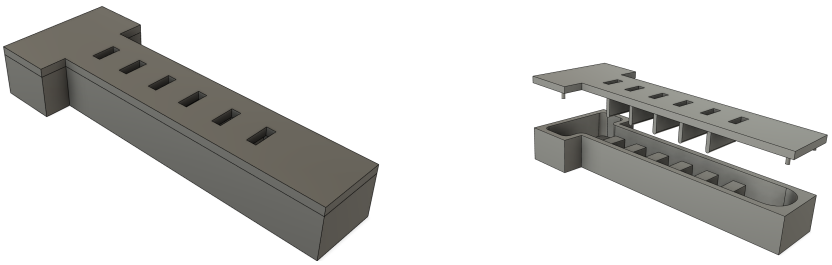

(a) (b)

Figure A.2: **These figure show the actuator chamber mold for Version 1. Of note is the lightweight construction of the top half of the mold which led to the mold breaking.**

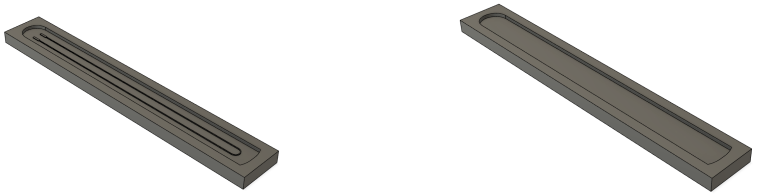

(a) (b)

Figure A.3: **The above figure shows the mold system used to create the bend sensor for Version 1 of the actuator. At this stage of the project, a separate mold was still being used to create the skin for the actuator.**

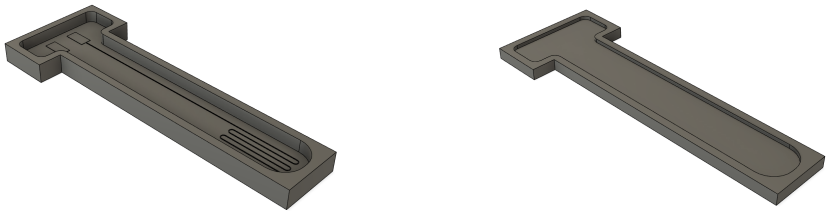

(a) (b)

Figure A.4: **he above figure shows the mold system used to create the force for Version 1 of the actuator. At this stage of the project, a separate mold was still being used to create the skin for the actuator.**

A.2 Version 2

A.2.1 Design

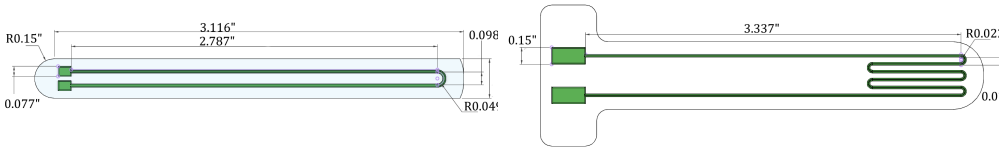

(a) (b)

Figure A.5: **The above figures show the drawings and dimensions for the top and bottom sensors of Version 2 of the actuator. In this version the sensor channel heights were made higher which is not reflected in this figure.**

A.2.2 Molds

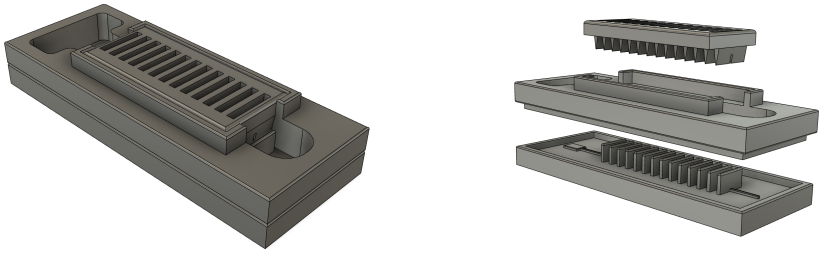

(a) (b)

Figure A.6: **Above is shown the molds needed to create the air chamber portion of Version 2. In this case it switched to three part mold. This was done in an effort to make the process of extracting the actuator from the molds much easier.**

(a) (b)

Figure A.7: **The version 2 top sensor molds were much the same as the as in version 1 but featured a heightened sensor channel. It also was constructed using thicker walls and more material to prevent warping.**

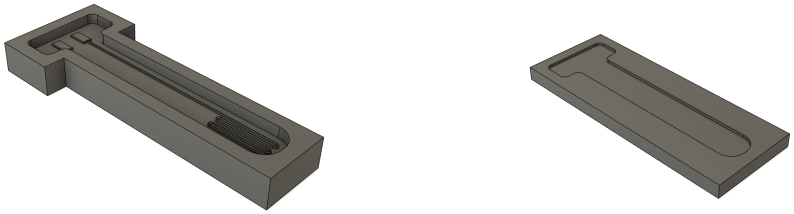

(a) (b)

Figure A.8: **The version 2 bottom sensor had higher sensor channels to prevent them from filling in when laminating parts together. It also was designed with thicker walls to prevent warping.**

A.3 SpinCoater Pieces

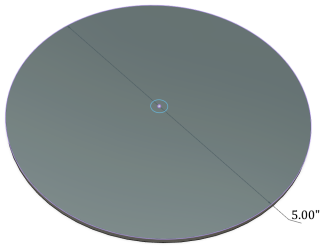

(a)

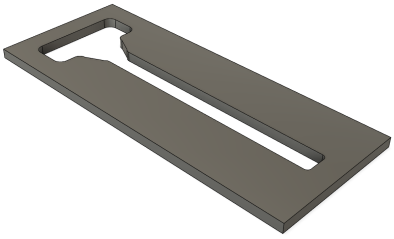

(b)

Figure A.9: **The left image (a) shows the acrylic disks used to create silicone skins to be used in constructing the actuator. The right (b) image shows an acrylic plate with a cutout matching the top sensor for version 3 of the design. This was used to spin coat uncured elastomer onto the top sensor for attaching the parts together in the final assembly.**

A.4 PCB Design

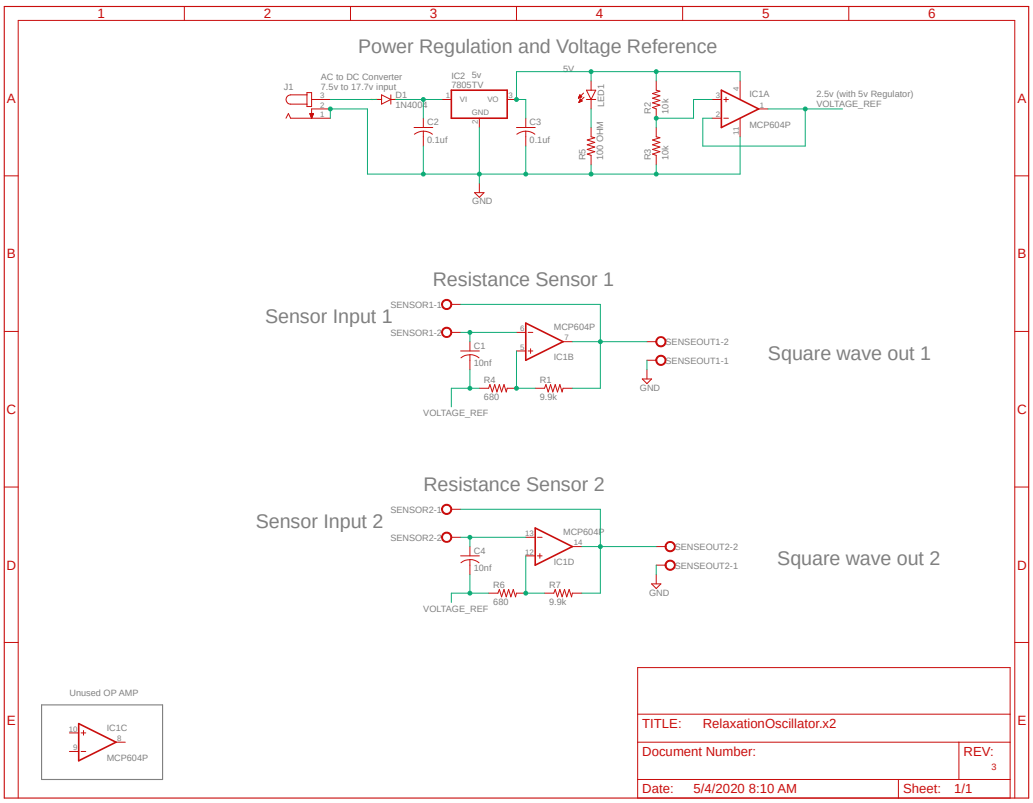

Figure A.10: **Shown is the schematic used to create the PCB for the relaxation oscillator.**

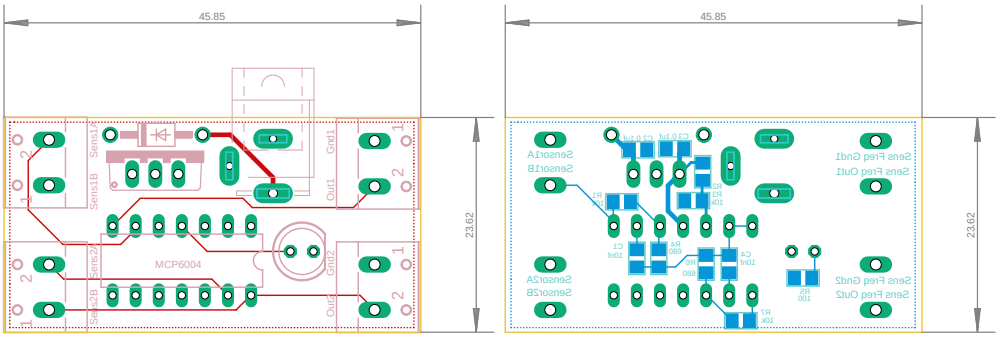

(a) (b)

Figure A.11: **Above are the top and bottom sides of the PCB created for the relaxation oscillator. For connectors a barrel jack was used to provide power from a 7v wall adapter. Screw terminals were chosen to connect to both the sensors and the Arduino.**

Bibliography

[1] *Arduino Nano*. Tech. rep. Arduino, Apr. 2020. URL: https://store.arduino.cc/usa/arduino-nano.

[2] M. Boivin, D. Milutinović, and M. Wehner. "Movement Error Based Control for a Firm Touch of a Soft Somatosensitive Actuator". In: *2019 American Control Conference (ACC)*. 2019, pp. 7–12.

[3] *BSP000W - BSP B010-EV002-A00A0B-S4*. Tech. rep. Balluff, Apr. 2020. URL: https://www.balluff.com/en/de/productfinder/product/?key=BSP000W#/.

[4] Jean-Baptiste Chossat et al. "A Soft Strain Sensor Based onIonic and Metal Liquids". In: *IEEE Sensors Journal* 13.9 (Sept. 2013), pp. 3405–3414.

[5] Matteo Cianchetti et al. "STIFF-FLOP Surgical Manipulator: mechanical design and experimental characterization of the single module". In: IEEE/RSJ International Conference on Intelligent Robots and Systems. Nov. 2013. URL: Tokyo,%20Japan.

[6] E. B. Dolan et al. "An actuatable soft reservoir modulates host foreign body response". In: *Science Robotics* 4 (Aug. 2019).

[7] *Dragon Skin 10*. Tech. rep. Smooth On, Apr. 2020. URL: https://www.smooth-on.com/products/dragon-skin-10-medium/.

[8] *Dragon Skin 30*. Tech. rep. Smooth On, Apr. 2020. URL: https://www.smooth-on.com/products/dragon-skin-30/.

[9] *Ecoflex^{TM} 00-30*. Tech. rep. Smooth On, Apr. 2020. URL: https://www.smooth-on.com/products/ecoflex-00-30/.

[10] *FlexiForce A502 Sensor*. Tech. rep. Tekscan, May 2020. URL: https://www.tekscan.com/products-solutions/force-sensors/a502.

[11] Google. *Google Books-Ngram Viewer-Soft Robot*. Apr. 2020. URL: https://books.google.com/ngrams/graph?content=soft+robot%5C&year_start=

1800%5C&year_end=2008%5C&corpus=15%5C&smoothing=0%5C&share=%5C&direct_url=t1%5C%3B%5C%2Csoft%5C%20robot%5C%3B%5C%2Cc0#t1%5C%3B%5C%2Csoft%5C%20robot%5C%3B%5C%2Cc1.

[12] Y. Hao et al. "Universal soft pneumatic robotic gripper with variable effective length". In: *2016 35th Chinese Control Conference (CCC)*. 2016, pp. 6109–6114.

[13] Andrea Lloyd. *Beyond the Metal: Investigating Soft Robots at NASA Langley*. May 2019. URL: https://www.nasa.gov/feature/langley/beyond-the-metal-investigating-soft-robots-at-nasa-langley.

[14] P. Maiolino et al. "Soft dielectrics for capacitive sensing in robot skins: Performance of different elastomer types". In: *Sensors and Actuators A: Physical* 226 (Feb. 2015), pp. 37–47.

[15] *MCP4725*. Tech. rep. Microchip, Apr. 2020. URL: https://www.microchip.com/wwwproducts/en/MCP4725.

[16] Selim Ozel et al. "A precise embedded curvature sensor module for soft-bodied robots". In: *Sensors and Actuators A: Physical* 236 (Oct. 2015), pp. 349–359.

[17] Y. Park, B. Chen, and R. J. Wood. "Design and Fabrication of Soft Artificial Skin Using Embedded Microchannels and Liquid Conductors". In: *IEEE Sensors Journal* 12.8 (2012), pp. 2711–2718.

[18] Stefania Russo et al. "Soft and Stretchable Sensor Using Biocompatible Electrodes and Liquid for Medical Applications". In: *Soft Robotics* 2.4 (Dec. 2015), pp. 146–154.

[19] R. F. Shepherd et al. "Multigait soft robot". In: *Proceedings of the National Academy of Sciences* 108.51 (2011), pp. 20400–20403. DOI: 10.1073/pnas.1116564108.

[20] Sigma-Aldrich. *1-Ethyl-3-methylimidazolium ethyl sulfate*. Tech. rep. Apr. 2020.

[21] *Silicone Thinner*. Tech. rep. Smooth On, Apr. 2020. URL: https://www.smooth-on.com/products/silicone-thinner/.

[22] *SLO-JO*. Tech. rep. Smooth On, Apr. 2020. URL: https://www.smooth-on.com/products/slo-jo/.

[23] *SMC ITV2030-31N3N4 regulator, electro-pneumatic, IT2000/ITV2000 E/P REGULATOR*. Tech. rep. SMC Pneumatics, Apr. 2020. URL: https://www.smcpneumatics.com/ITV2030-31N3N4.html.

[24] G. Soter et al. “Skinflow: A soft robotic skin based on fluidic transmission”. In: *2019 2nd IEEE International Conference on Soft Robotics (RoboSoft)*. 2019, pp. 355–360.

[25] *THE BEND SENSOR®*. Tech. rep. FlexPoint, May 2020. URL: `https://www.flexpoint.com/bend-sensor`.

[26] *The mGrip Ecosystem*. Tech. rep. Soft Robotics Inc. URL: `https://www.softroboticsinc.com/products/mgrip/`.

[27] Michael T. Tolley et al. “A Resilient, Untethered Soft Robot”. In: *Soft Robotics* 1.3 (Sept. 2014).

[28] Ryan L. Truby et al. “Soft Somatosensitive Actuators via Embedded 3D Printing”. In: *Advanced Materials* 30.15 (Apr. 2018).

[29] Lucie Viry et al. “Flexible Three-Axial Force Sensor for Soft and Highly Sensitive Artificial Touch”. In: *Advanced materials* 26 (May 2014), pp. 2659–2664.

[30] Z. Wang, Y. Torigoe, and S. Hirai. “A Prestressed Soft Gripper: Design, Modeling, Fabrication, and Tests for Food Handling”. In: *IEEE Robotics and Automation Letters* 2.4 (2017), pp. 1909–1916.